# Advanced measurement techniques for high Re-number testing and CFD validation

Dr. Lars Koop

DLR, German Aerospace Center
Institute of Aerodynamics and Flow Technology
**Experimental Methods**


DLR



## Introduction 1/2

General topic: Advanced measurement techniques

**Mission**: Development of **optical and acoustical field measurement techniques** for the acquisition of fluid-mechanical and aero-acoustical quantities.
Application mainly in **large industrial wind tunnels** and at **in-flight testing** for aerodynamics.
**Objective**: Quality of the results obtained is comparable with the results attained in the laboratory.

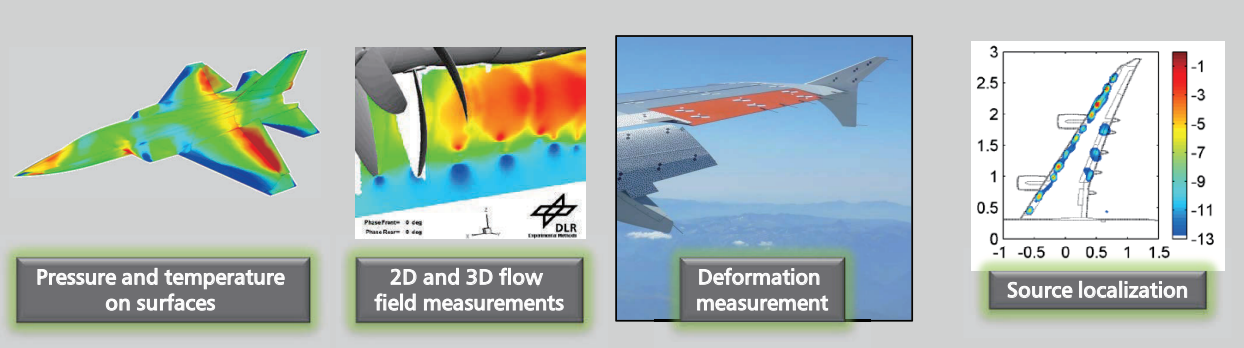


DLR

# Introduction 2/2: Overview

CFD validation and High Re-number testing

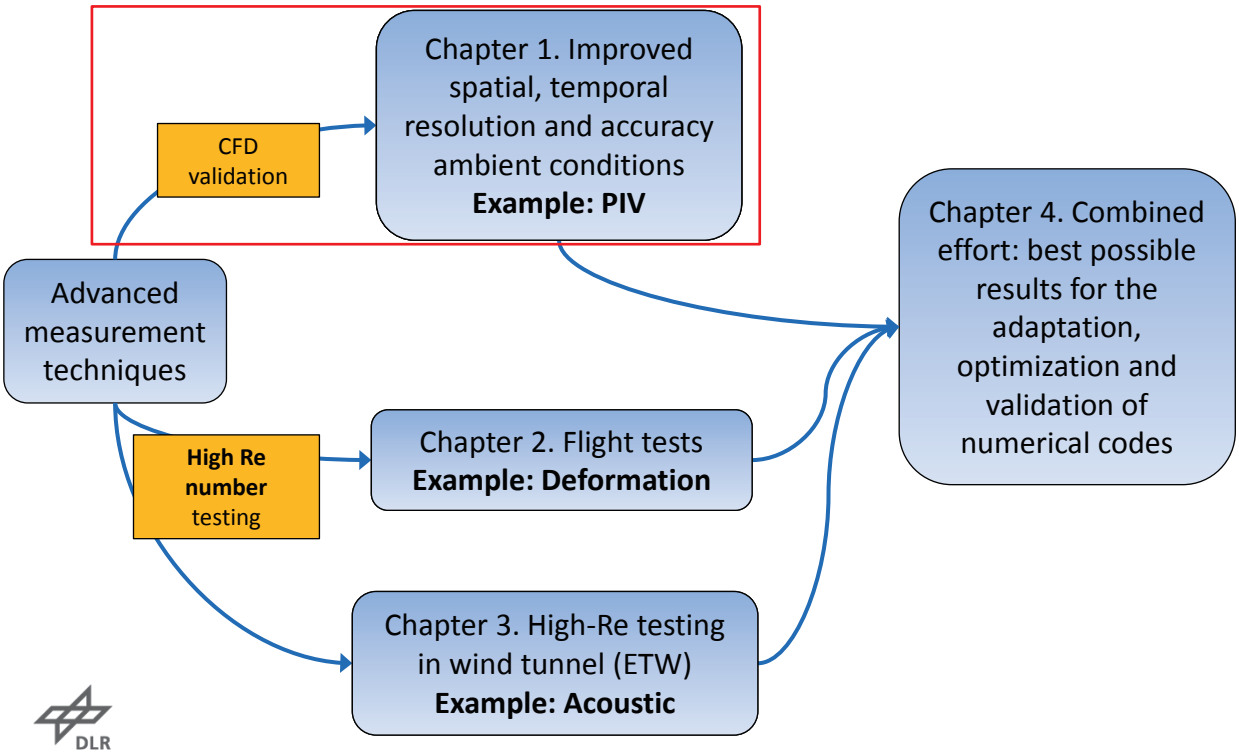




# Improved spatial and temporal resolution for CFD validation

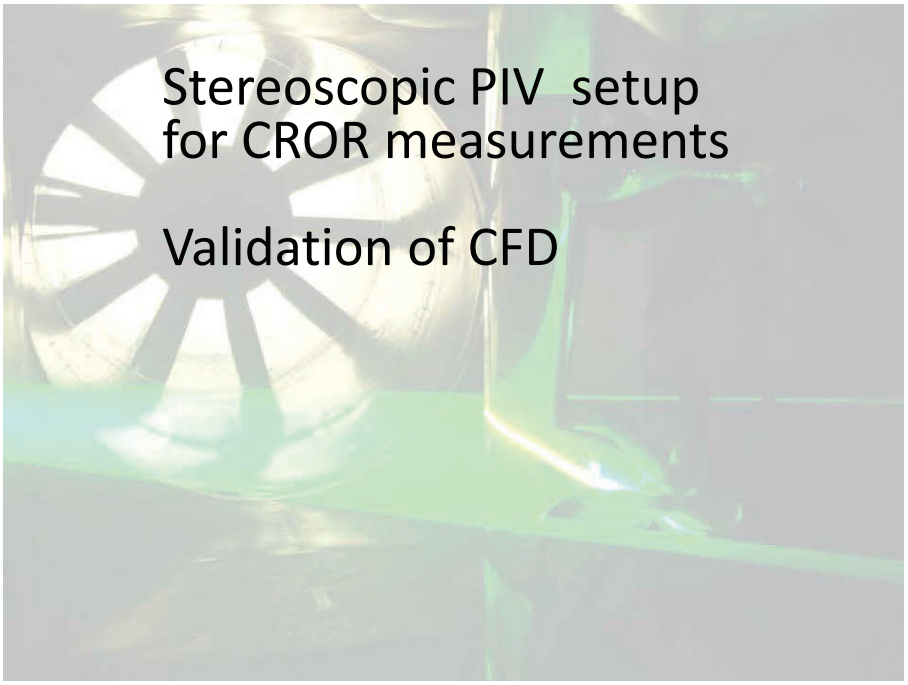

DLR.de • Chart 5 > L. Koop • High-Re Testing > July 7th 2016

## PIV measurements at AIRBUS (BLSWT)

### Counter-Rotating Open Rotor (CROR) measurements

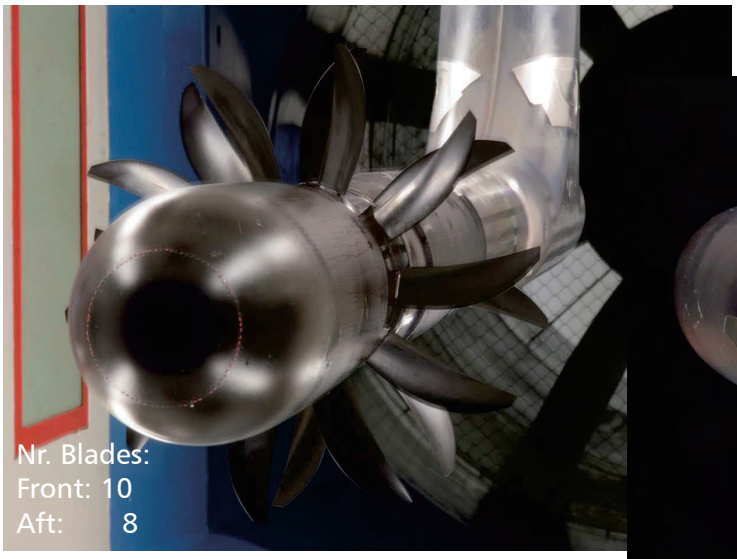


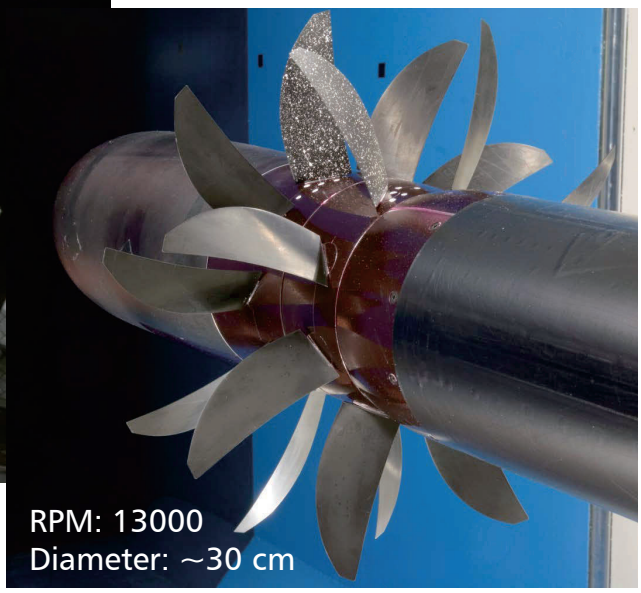


DLR.de • Chart 6 > L. Koop • High-Re Testing > July 7th 2016

## PIV measurements at AIRBUS (BLSWT)

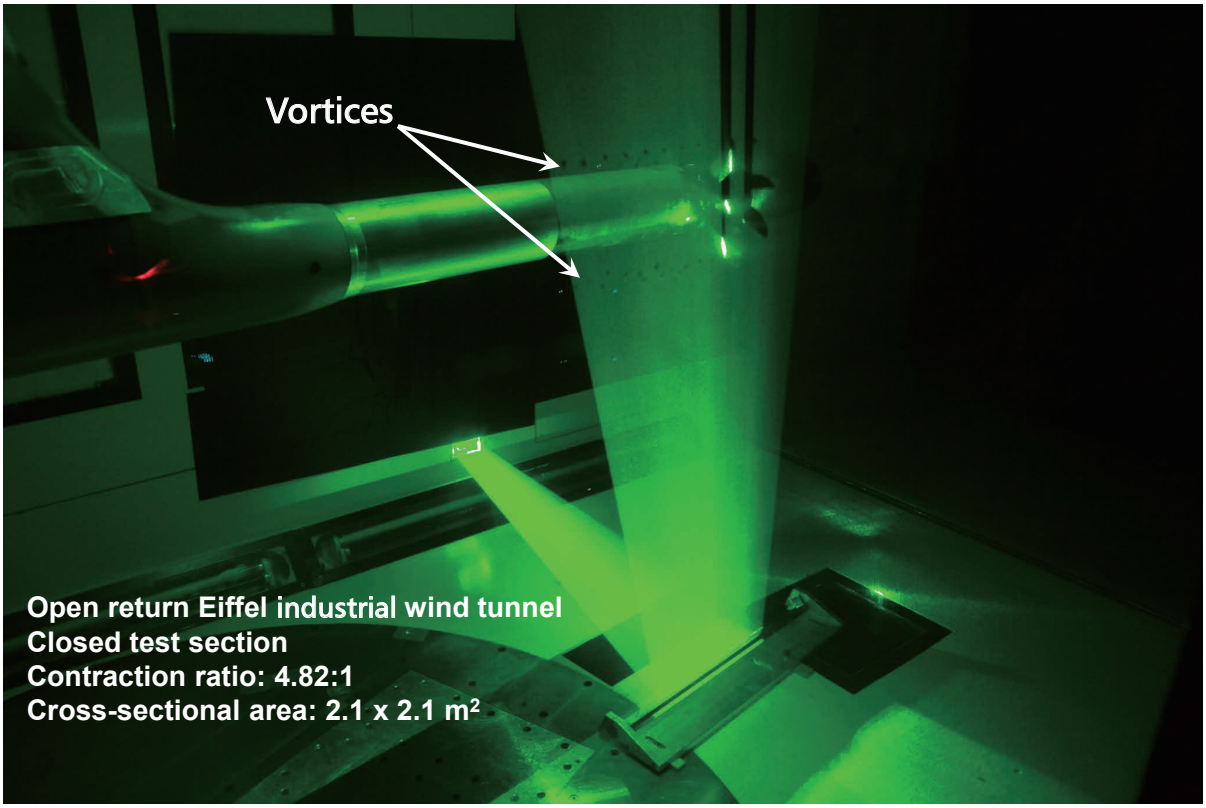

# PIV measurements at AIRBUS (BLSWT)

## Phase averaged PIV results

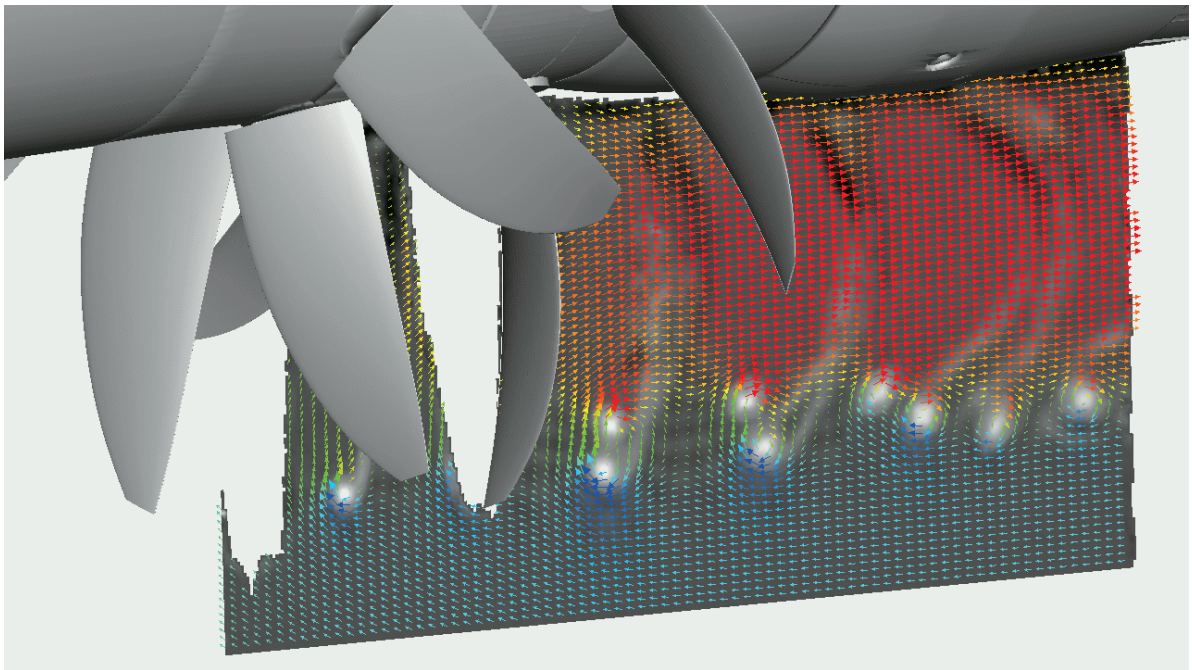



# PIV measurements at AIRBUS (BLSWT)

## Comparison between experiment and CFD

- Favorable agreement between PIV and CFD
- Tip vortex characteristics and trajectories well matched (CFD optimized in near blade region)
- Interactions of the front and aft blade vortices downstream of the rear rotor agree in CFD and PIV results
- However, CFD mesh coarsens with increasing axial distance from rotors, thus the vortices dissipate more rapidly than measured

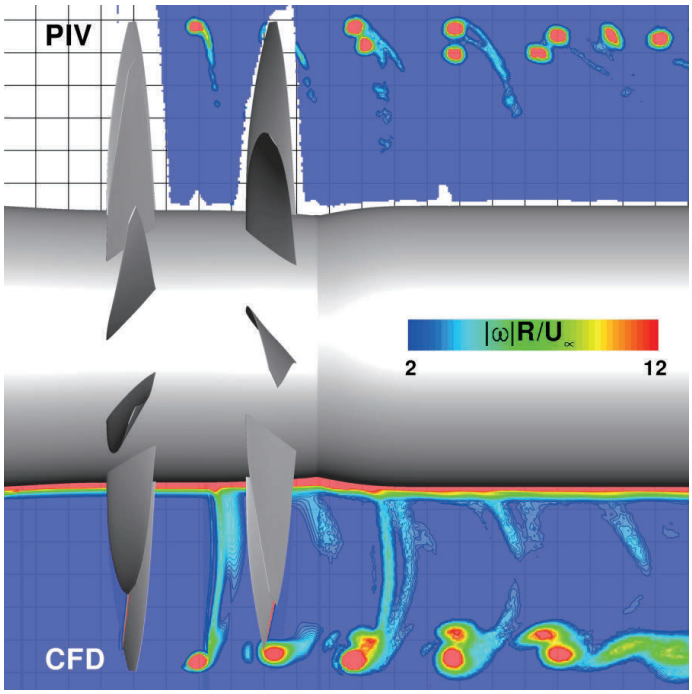

# PIV measurements at AIRBUS (BLSWT)

Comparison between experiment and CFD

- Slight offset in radial position visible between CFD and PIV
- **CFD shows slightly more inboard location**, slipstream contraction, (blade loading) might be higher
- Consistent with observed **higher velocity magnitude** in the CFD simulations
- Caused by **differences in blade pitch**, i.e. rigid in CFD, flexible in experiment (IPCT)

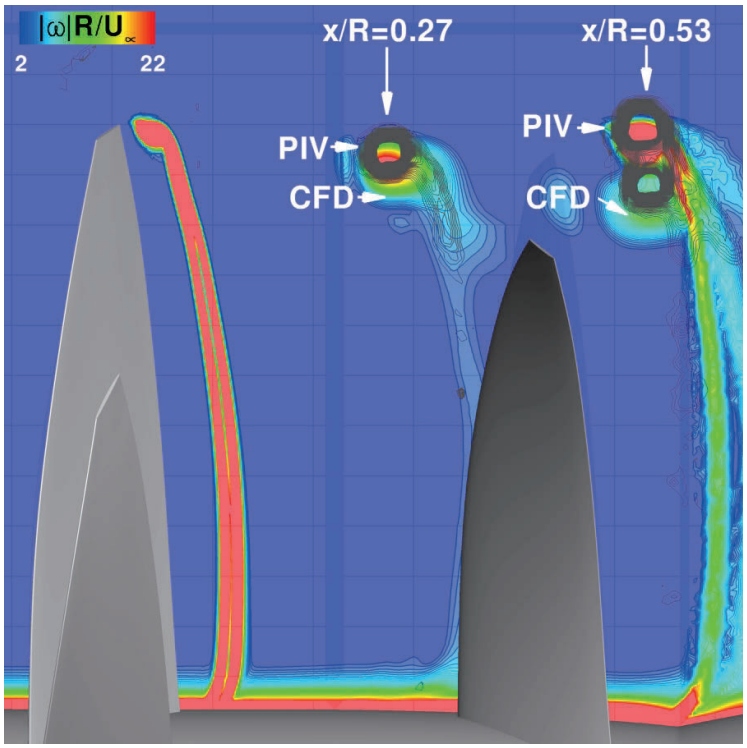




# IPCT measurements at AIRBUS (BLSWT)

CROR model IPEKA

- Deformation of front and rear propeller measured in separate sequences
  → Phase-locked position of measured propeller
- Laser illumination to enable short exposure time
- Random dot pattern painted on the propeller blades
- Additional reference markers as undeformed reference to be fixed for the evaluation of the deformation

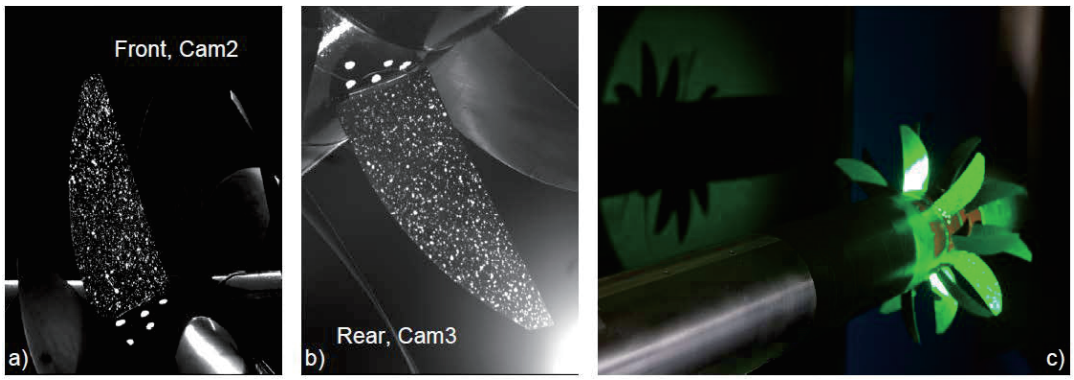

# Improved spatial and temporal resolution for CFD validation Step 2: Tomo-PIV

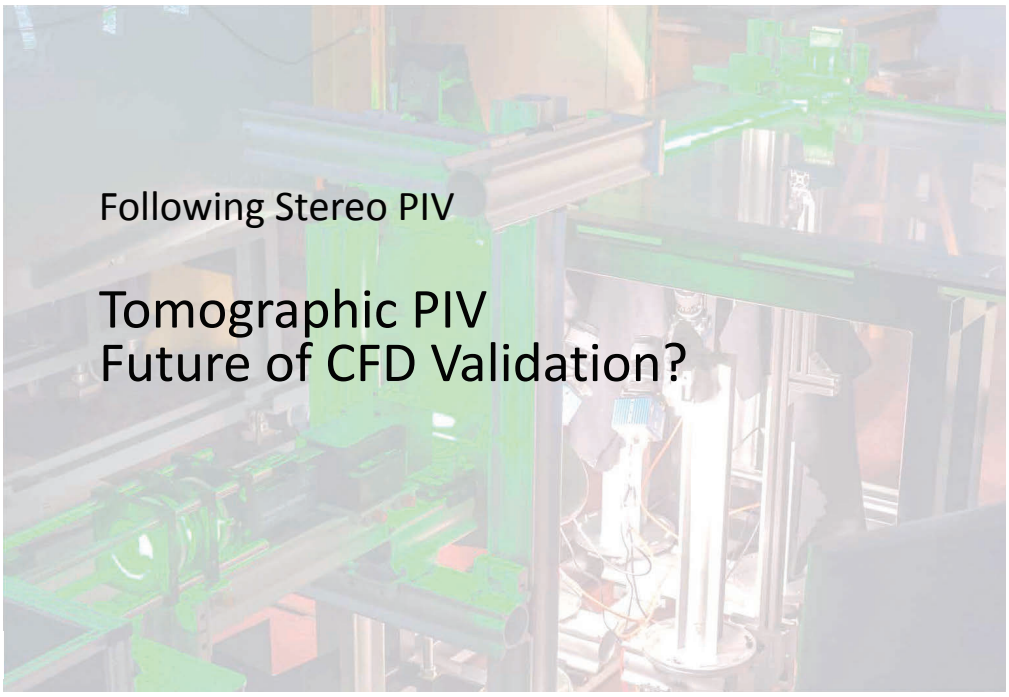


DLR



# Stereo PIV -- What comes next?

- Restrictions of Stereo PIV:
  - Flow velocity in two dimensional plane
  - Spatial filtering/averaging due to interrogation windows
- Tomo-PIV
  - Flow velocity information in a volume
  - But:
    - We will see …

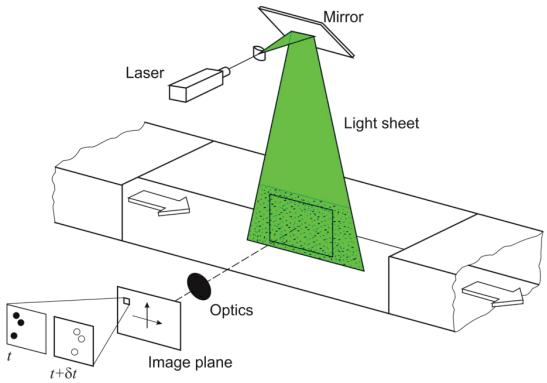


Interrogation window

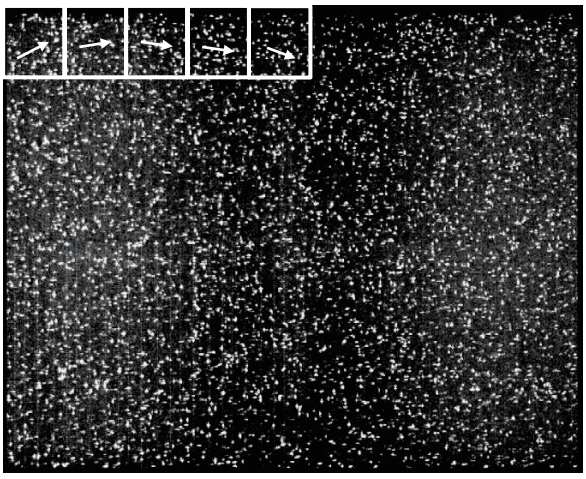

DLR

# Tomographic PIV

## Working principle

- Fully three dimensional time resolved flow field
- Thick light sheet illuminated by high repetition rate laser
- Scattered light recorded by 4 high-speed cameras
- Image to object 3D mapping function (+self-calibration)
- MART (multiplicative algebraic reconstruction technique)
- Tomographic reconstruction of particle images
- Local 3D cross-correlation
- Time series of 3D-3C velocity information

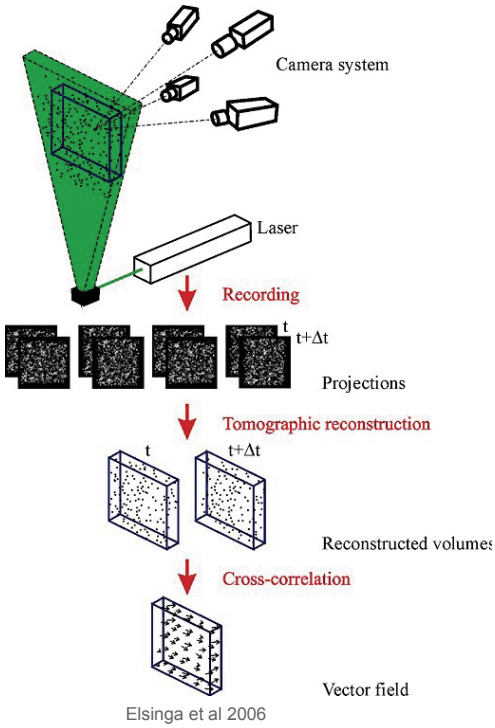




# Tomographic PIV – BFS measurements

## Backward facing step

- Development of velocity profile
- Formation of laminar separation bubble behind step
- Occurrence of spanwise 2D roller waves (KH - instabilities)
- Breakup into three-dimensional structures
- Reattachment and anew formation of profile

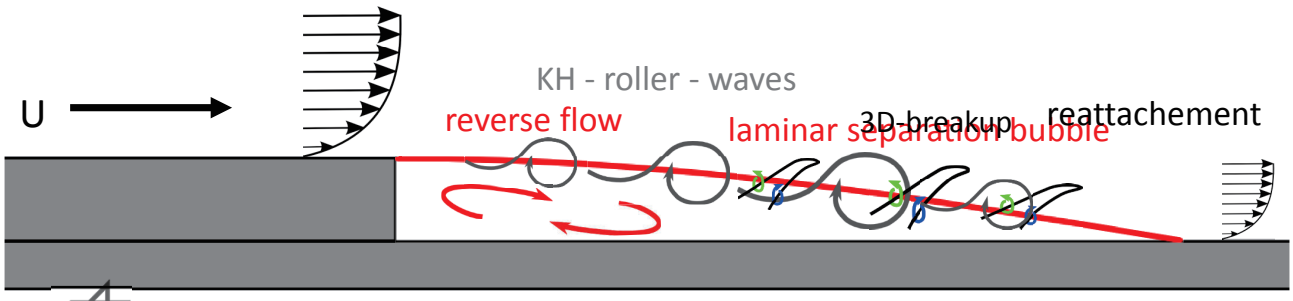

# Tomographic PIV – BFS measurements

## The model

- Elliptical leading edge
- Model on glass plate:
  - 190 mm inclined ramp leading to h = 6mm
  - 50 mm flat plate
- TOMO volume: 70 x 95 x 7 mm, 10 mm downstream of step
- Camera setup: below glass plate, pyramidal configuration

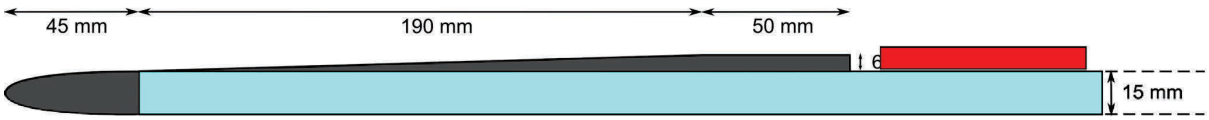




# Tomographic PIV – BFS measurements

## Experimental setup

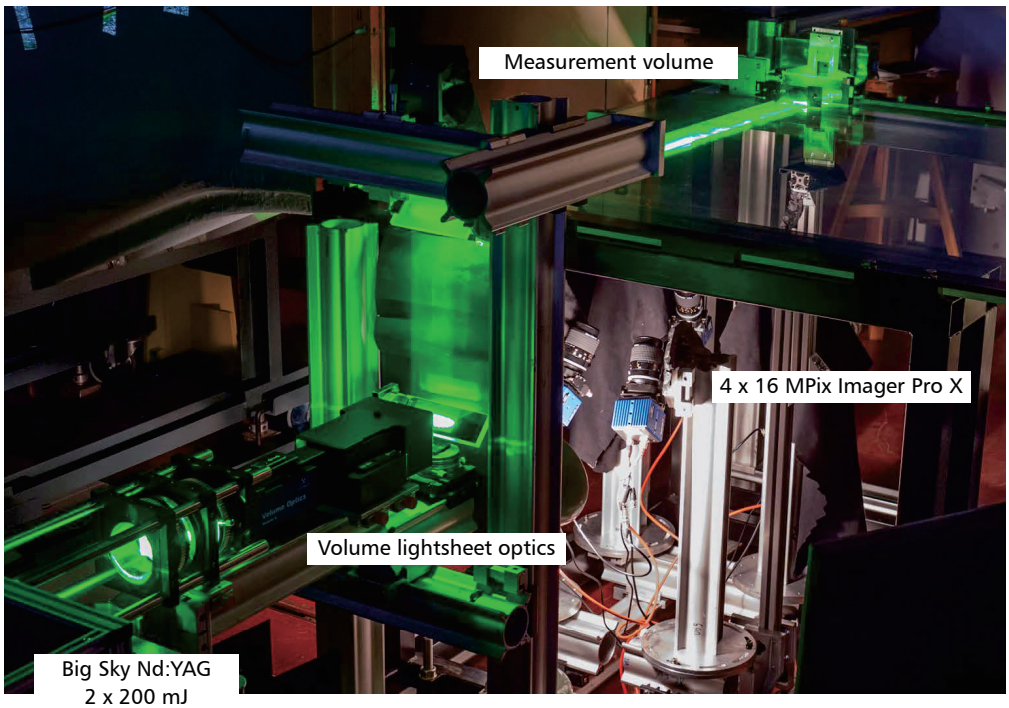

DLR.de • Chart 17 > L. Koop • High-Re Testing > July 7th 2016

# Tomographic PIV – BFS measurements

## Experimental setup

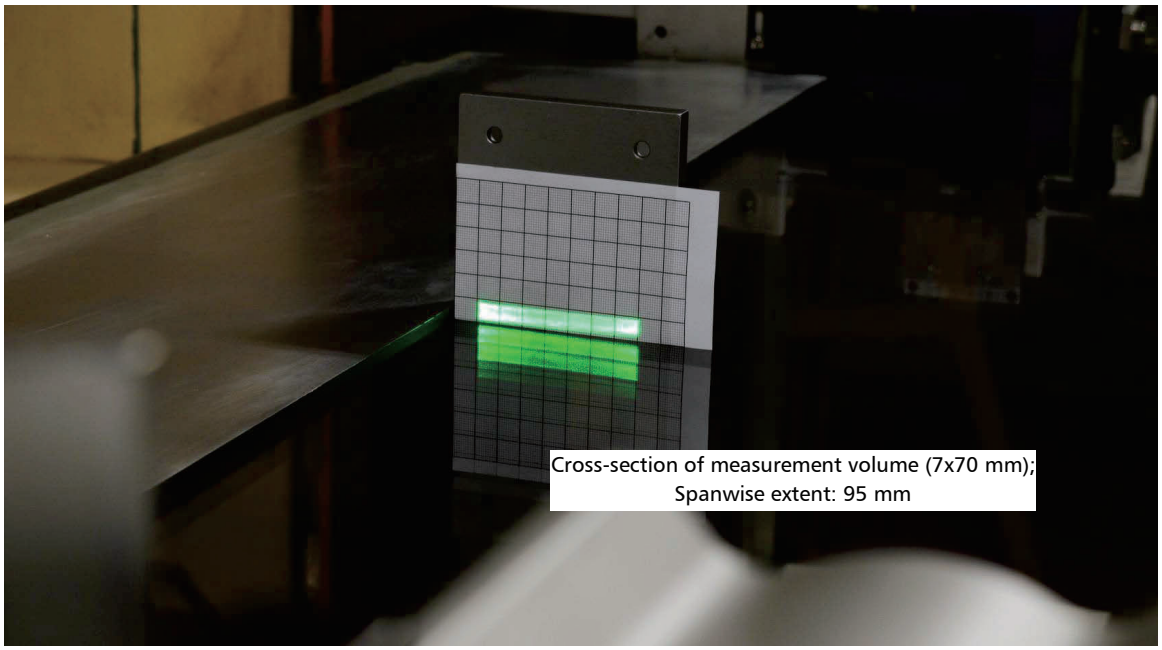


DLR

DLR.de • Chart 18 > L. Koop • High-Re Testing > July 7th 2016

# Tomographic PIV – BFS measurements

## Result

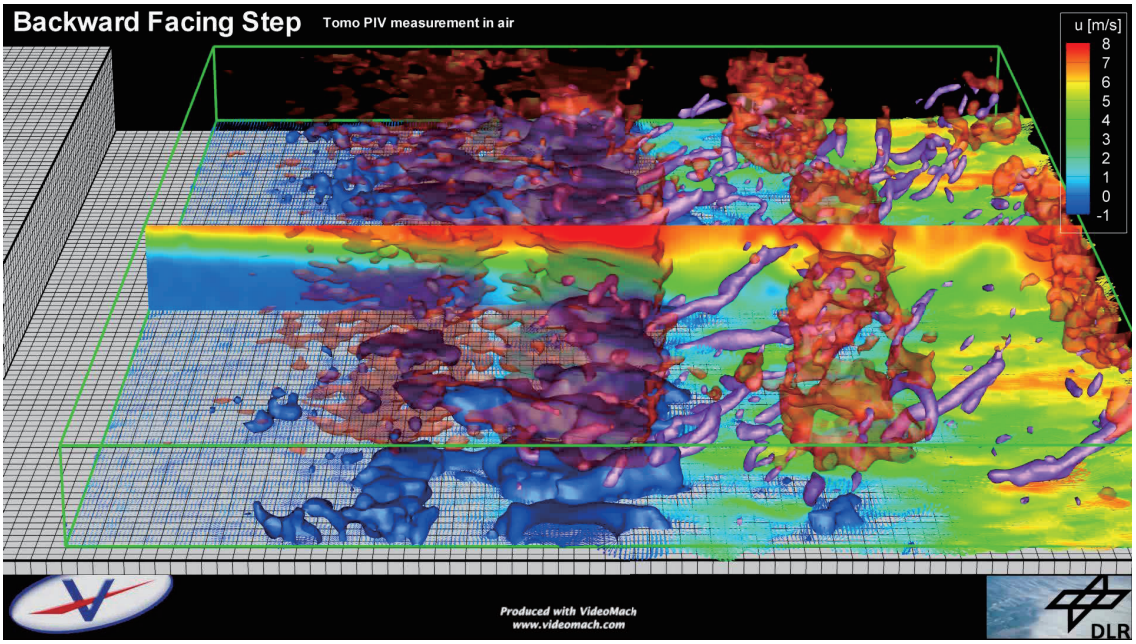


DLR

# Improved spatial and temporal resolution for CFD validation

## Advantages and limitations

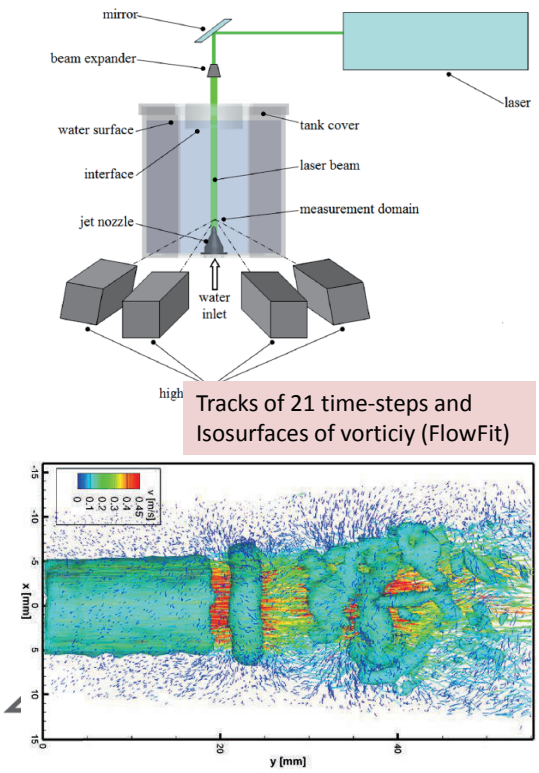


Images from multiple cameras are used to reconstruct the 3D particle field (**tomographic reconstruction**)

✓Flow velocity information in a volume

×spatial filtering/averaging

×computational cost

×ghost particle problem

×powerful illumination required



# Tomographic PIV

## The ghost particles

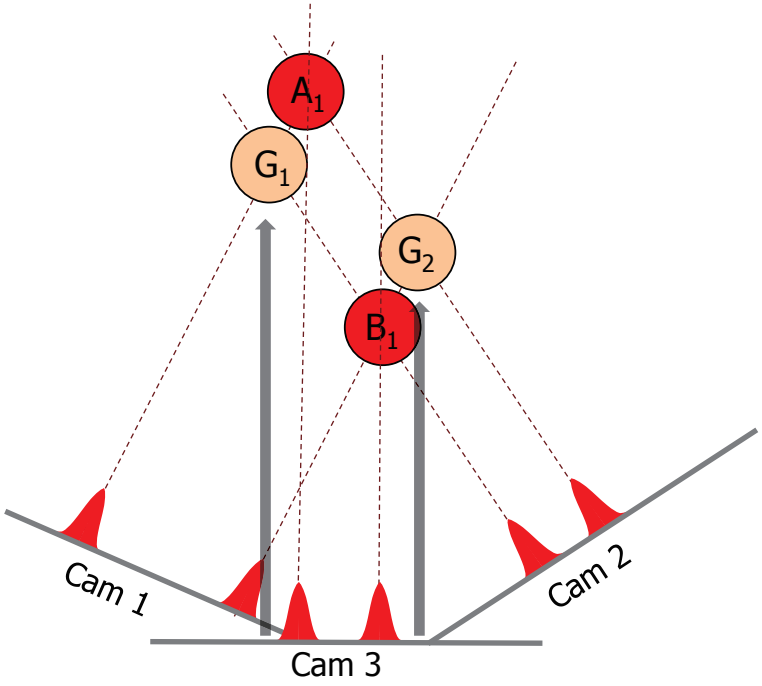


✓increase number of cameras

×increase costs

×increase setup complexity

×limited optical access

DLR

DLR.de • Chart 21 > L. Koop • High-Re Testing > July 7th 2016

# Tomographic PIV

## Volume illumination

Depth of field:

$$\delta z = 4.88 f_{\#}^{2} \left( \frac{M+1}{M} \right)^{2} \lambda$$

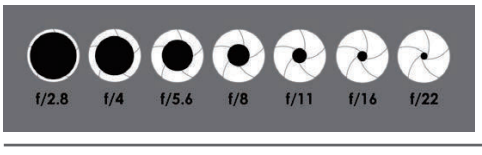


particles in focus

Image intensity decreases

Expanding the laser beam causes a decrease of light intensity

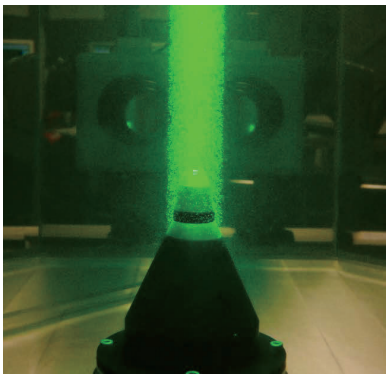

Violato et al 2011

Light amplification based on multi-pass reflections

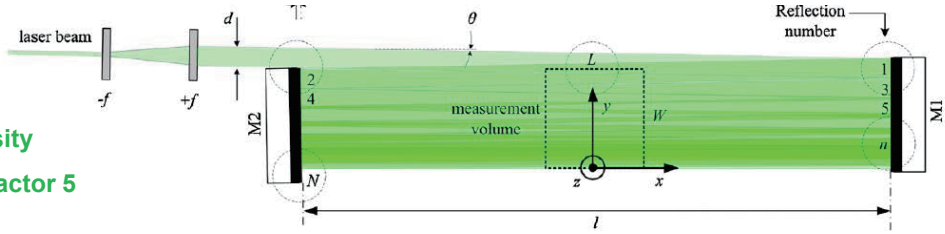


light intensity increased by factor 5

Ghaemi & Scarano 2010

DLR

DLR.de • Chart 22 > L. Koop • High-Re Testing > July 7th 2016

# Stereo PIV -- What comes next?

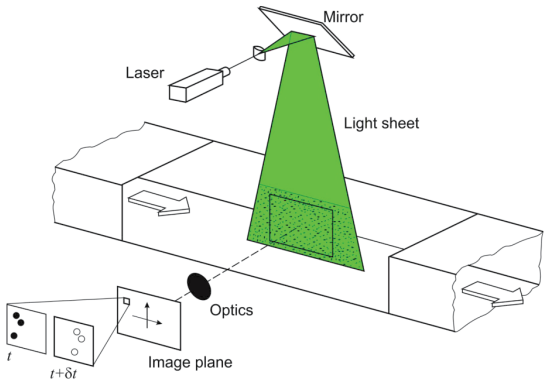


- Restrictions of Stereo PIV:
  - Flow velocity in two dimensional plane
  - Spatial filtering/averaging due to interrogation windows
- Tomo-PIV
  - Flow velocity information in a volume
  - But:
    - Spatial filtering/averaging
    - Very high computational cost
    - Ghost particle problem
    - Powerful illumination required
- Standard Particle Tracking Velocimetry (PTV)
  - 3D velocity information of a particle
  - But:
    - Only moderate seeding densities
    - Ghost particle problem
- Novel PTV technique: *Shake-The-Box*

Interrogation window

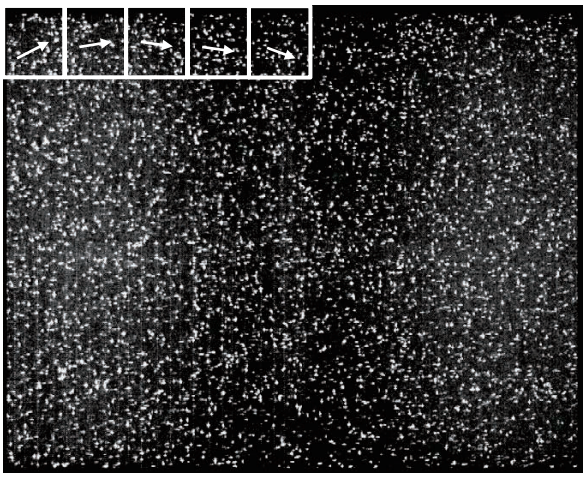

DLR

# Improved spatial and temporal resolution for CFD validation Step 3: Novel PTV Techniques

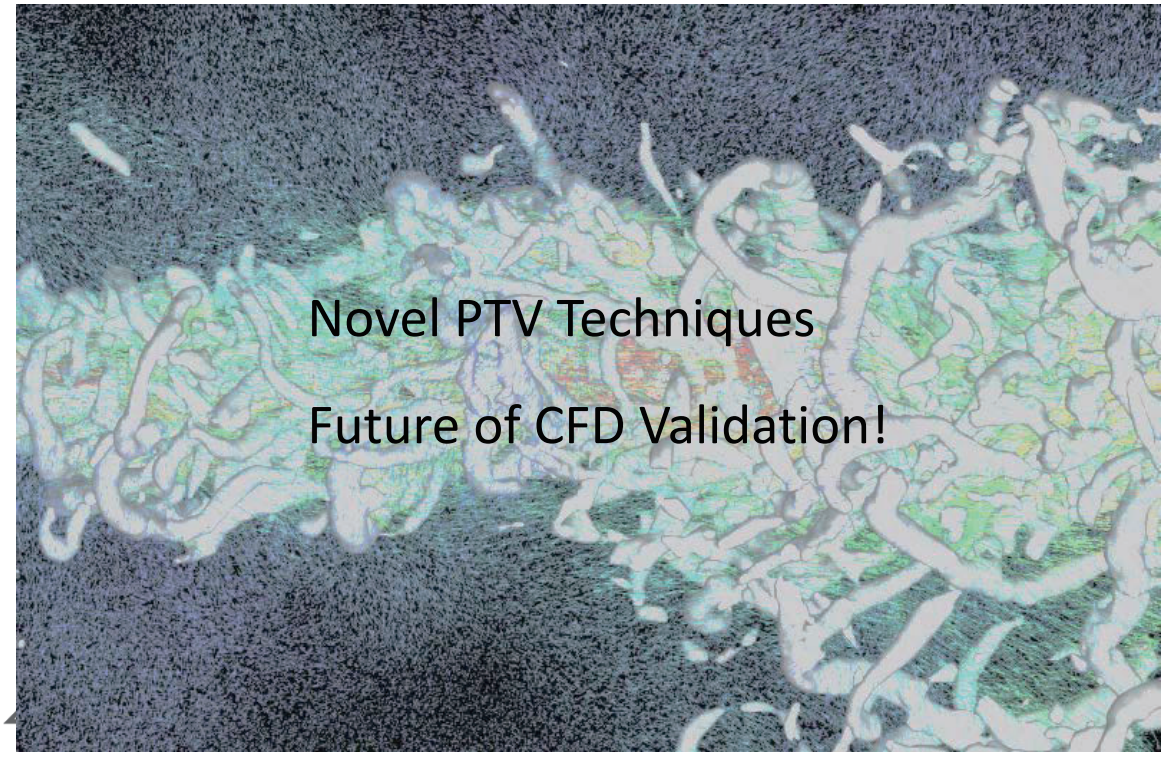




## Shake The Box (Schanz et al 2013)

**Particle based** reconstruction of trajectories → objects are represented by particle locations **no interrogation volumes (voxels)**

1. Perform standard Tomo-PIV reconstruction for initial time steps
2. Time resolved data: Knowledge of tracks allows prediction of next time step
   a. fit curve to time-steps *n-k* to *n*

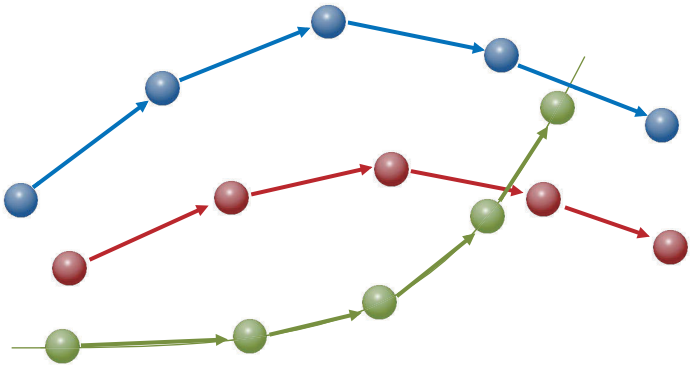

4-step tracks with low deviation from fit

DLR

## Shake The Box (Schanz et al 2013)

**Particle based** reconstruction of trajectories → objects are represented by particle locations (**no voxels**)

1. Perform standard Tomo-PIV reconstruction for initial time steps
2. Time resolved data: Knowledge of tracks allows prediction of next time step
   a. fit curve to time-steps *n-k* to *n*
   b. Extrapolate to *n+1*
   c. *Shake predicted particles*
   d. If significant number of tracks are known good prediction of particle distribution in next time step

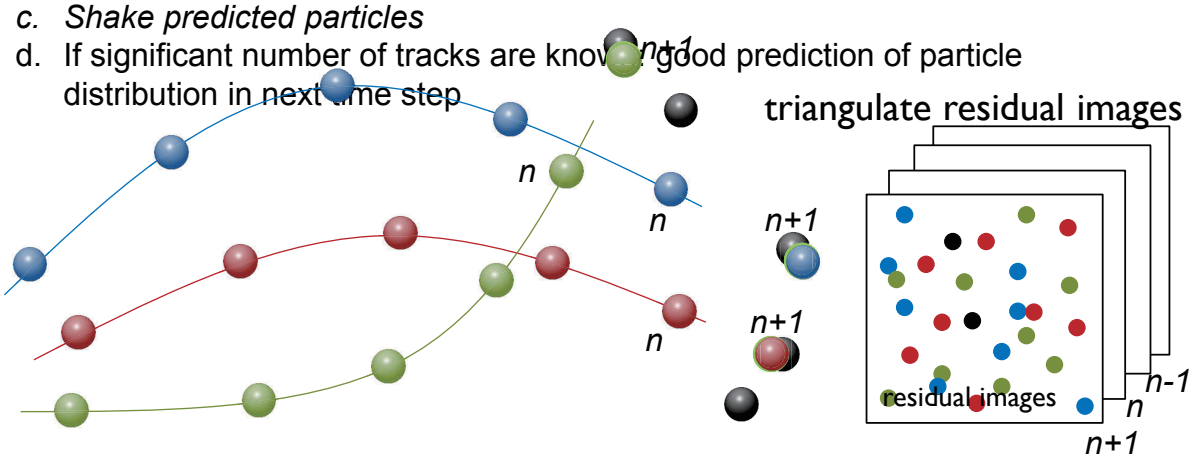


**Particle tracking with high seeding density and high accuracy, no ghost particles and low computational costs**



## Application of STB on tubulent boundary layer flow

- 1 meter wind tunnel Göttingen
- Velocity: 10 m/s
- Measurement volume:
  - **16 * 1.5 * 16 mm³** (y wall-normal)
- **4 * PCO dimax cameras at 15.9 kHz each**
- Resolution: 528 x 420 pixels, 30 mm/px
- 115300 successive images per run
- Up to 5600 particles per frame

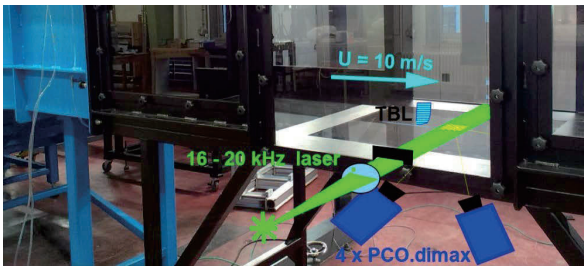


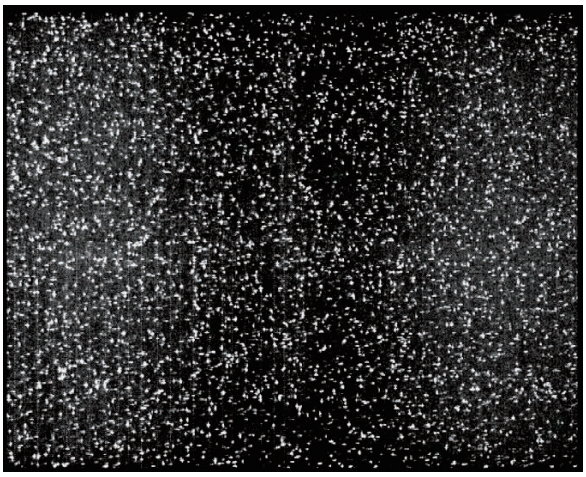

Exemplary camera image

## Application of STB on tubulent boundary layer flow

- Preliminary results
- Shown are particles for one time instance, followed by a seven-time-step trail
- Bin averaging of the particle properties allows for the generation of profiles with high spatial resolution (below 1/10 pixel)

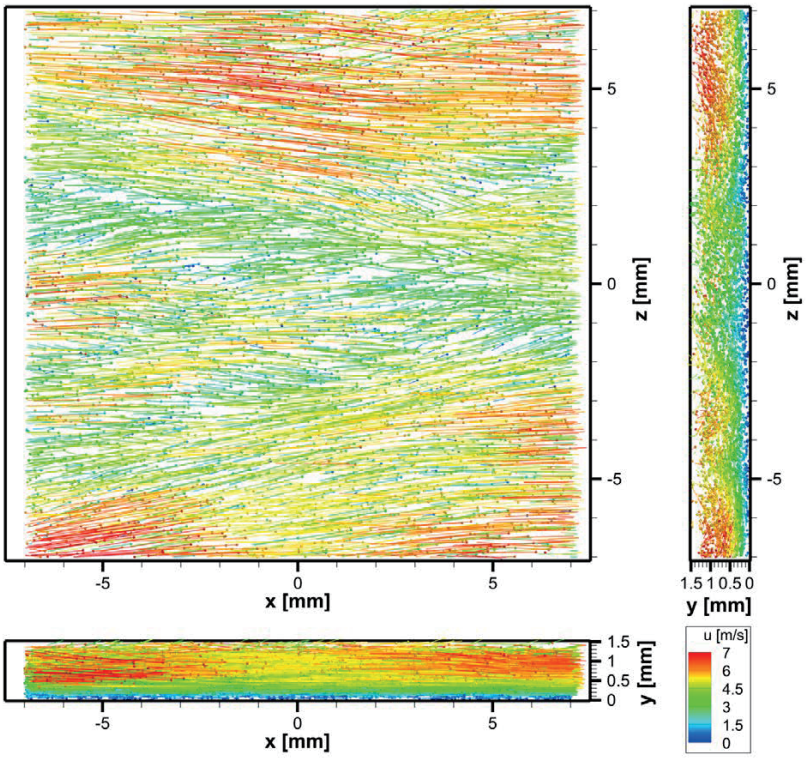




## TBL: Profiles of Reynolds stresses

- Very good agreement to DNS
- Unprecedented accuracy and resolution
- Non-intrusive
- No band-pass filtering due to binning

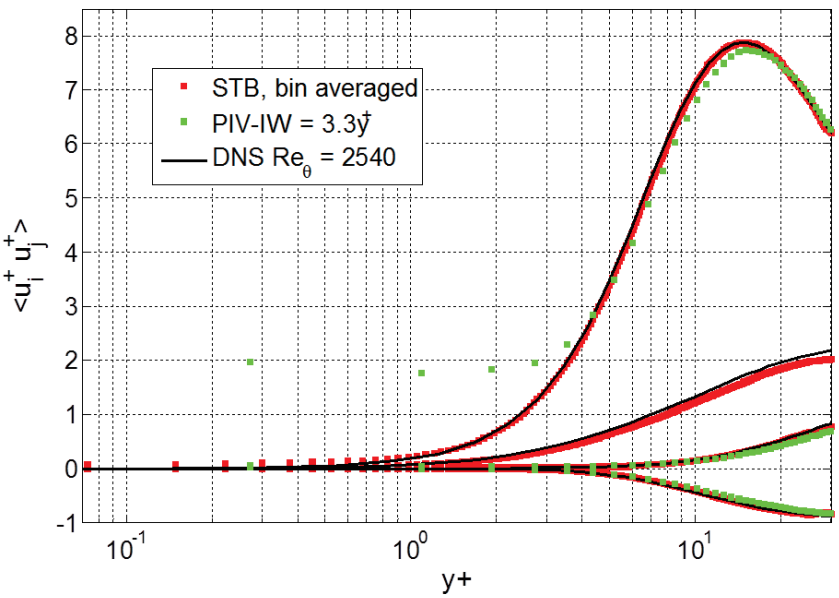


High-magnification 2C PIV-measurement

Shake-The-Box 3D particle tracking

## Experimental setup of large-scale thermal plume with HFSB

5x PCO Edge scientific CMOS
Close to in-line geometry
30Hz
f = 35mm
f# = 11
Resolution 2560 x 2160 px @ 16 bit

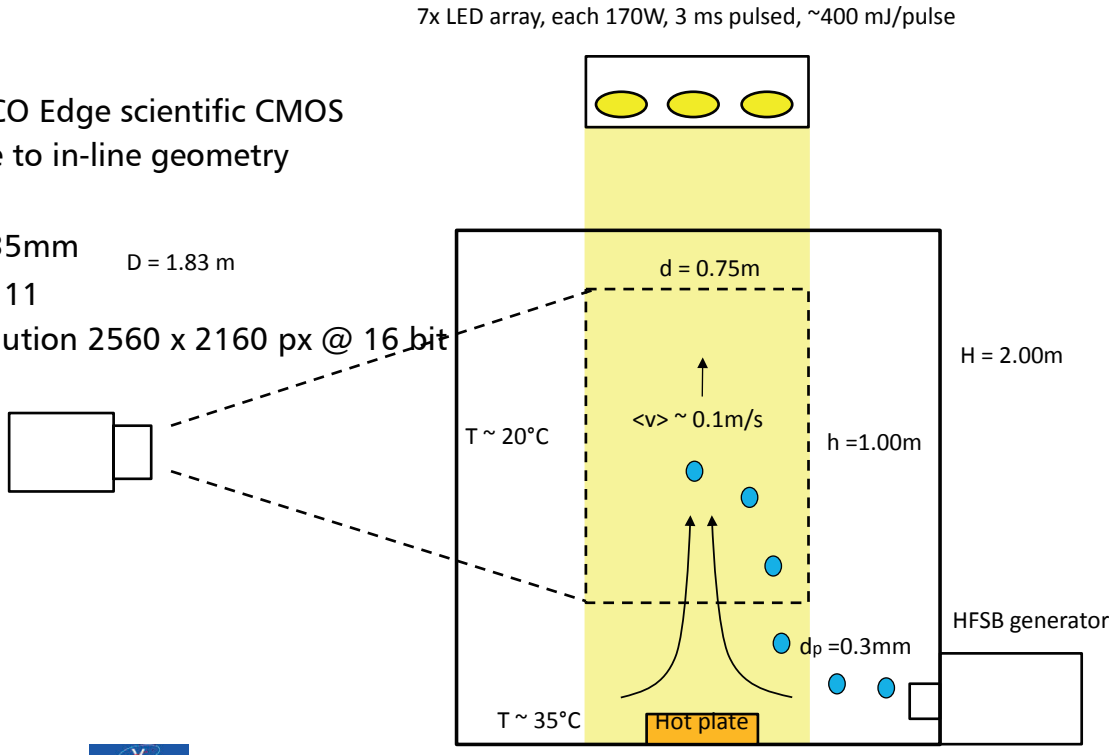


## STB results of thermal plume with HFSB

ppp ~ 0.1
(side to middle section)

~280,000 tracked particles per time step

Up to 3,000 time steps

Sphere for each particle

Color coding: streamwise velocity

**STB won the PIV-Challenge in 2014 for cases C and D**

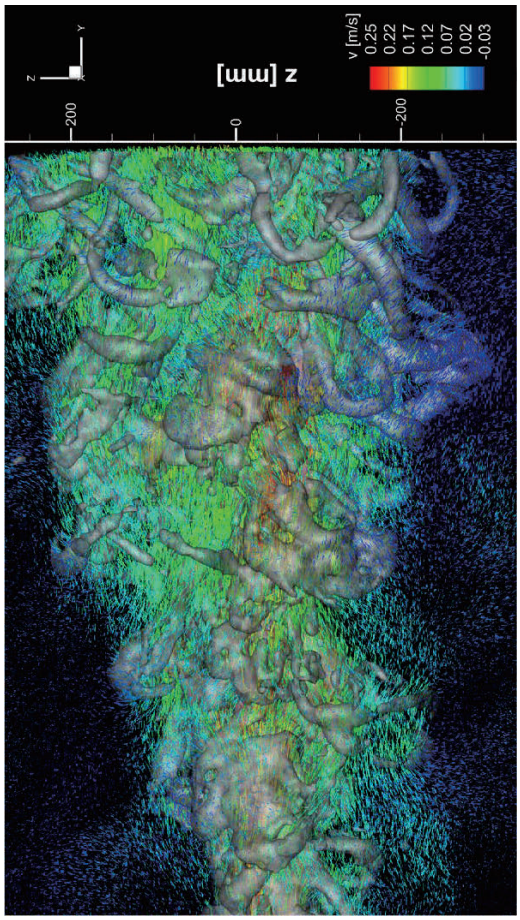

## Thermal plume, seeded by Helium filled soap bubbles

Volume: ~ 1m³
15°temperature difference
5 cameras at 30 Hz
STB: 270,000 bubble tracked simultaniously

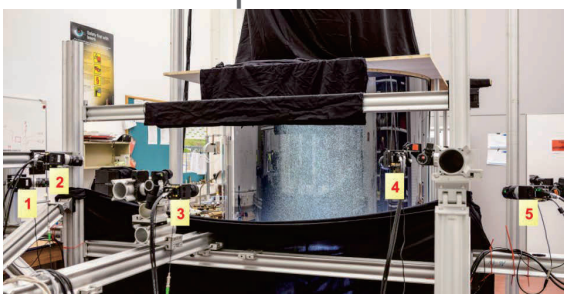


Soap bubbles, illuminated by LED

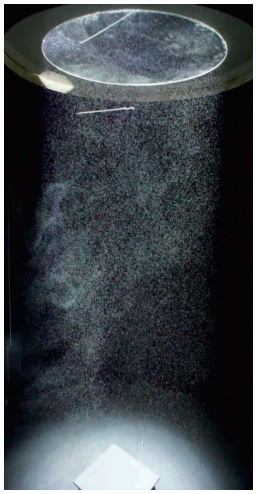

STB: Lagrangian particle tracks

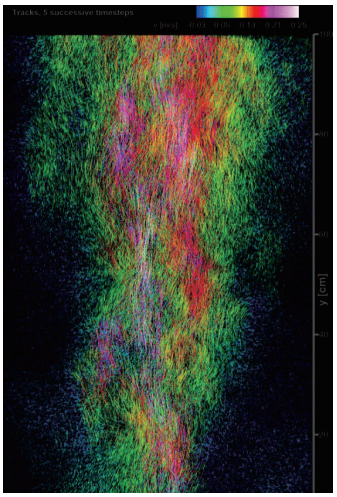

FlowFit: Eulerian grid from track velocity

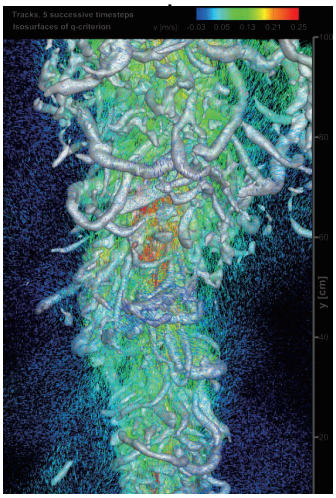

FlowFit: Eulerian grid from track acceleration

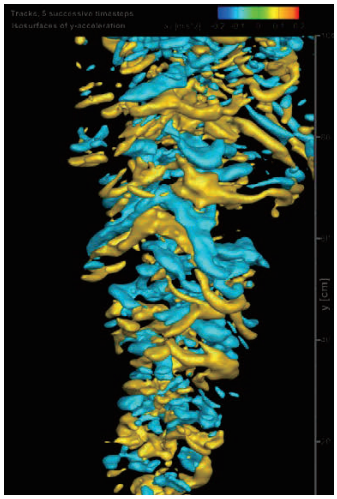



## Comparison of 3D measurement methods

| | Classic 3D PTV | TOMO-PIV | Shake-The-Box |
|---|---|---|---|
| Max. particle density | < 0.01 ppp | 0.1 ppp | 0.1 ppp |
| Lagrangian data | ✓ | ✗ | ✓ |
| Eulerian data | ✗ | ✓ | ✓ |
| Ghost particles | High | Medium | None |
| Accuracy | Medium | Medium | High |
| Acceleration calc. | Intrinsic | Indirect | Intrinsic |
| Calculation time | Low | Very high | Low |
| Memory req. | Low | Very high | Low |
| High speed flows | ✗ | ✓ | ( ✓)* |

DLR

DLR.de • Chart 33 > L. Koop • High-Re Testing > July 7th 2016

## Summary; Chapter 1

Improved spatial, temporal resolution and accuracy (ambient condition)

- **Advanced optical measurement techniques offer:**
  - Efficient measurements not only in research laboratories but in **industrial test facilities** as well
  - **High accuracy and high level of adaptation** (mobile systems)
  - High quality experimental data sets as required **for numerical code validation** and as boundary conditions for CFD
- Development towards **improved resolution measurement with optimal accuracy is mandatory** for optical non intrusive measurement techniques
  - New PTV Techniques: Future of CFD Validation!

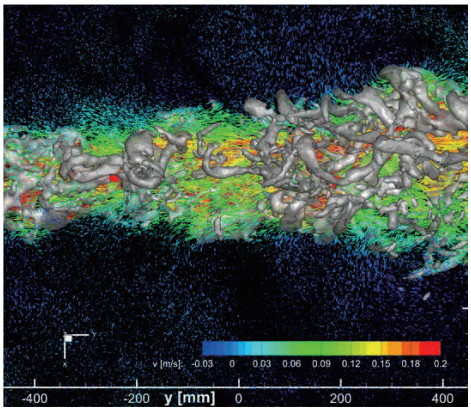


**Ambient condition W/T !**

DLR

DLR.de • Chart 34 > L. Koop • High-Re Testing > July 7th 2016

## Introduction 2/2: Overview

High Re-number testing and CFD validation

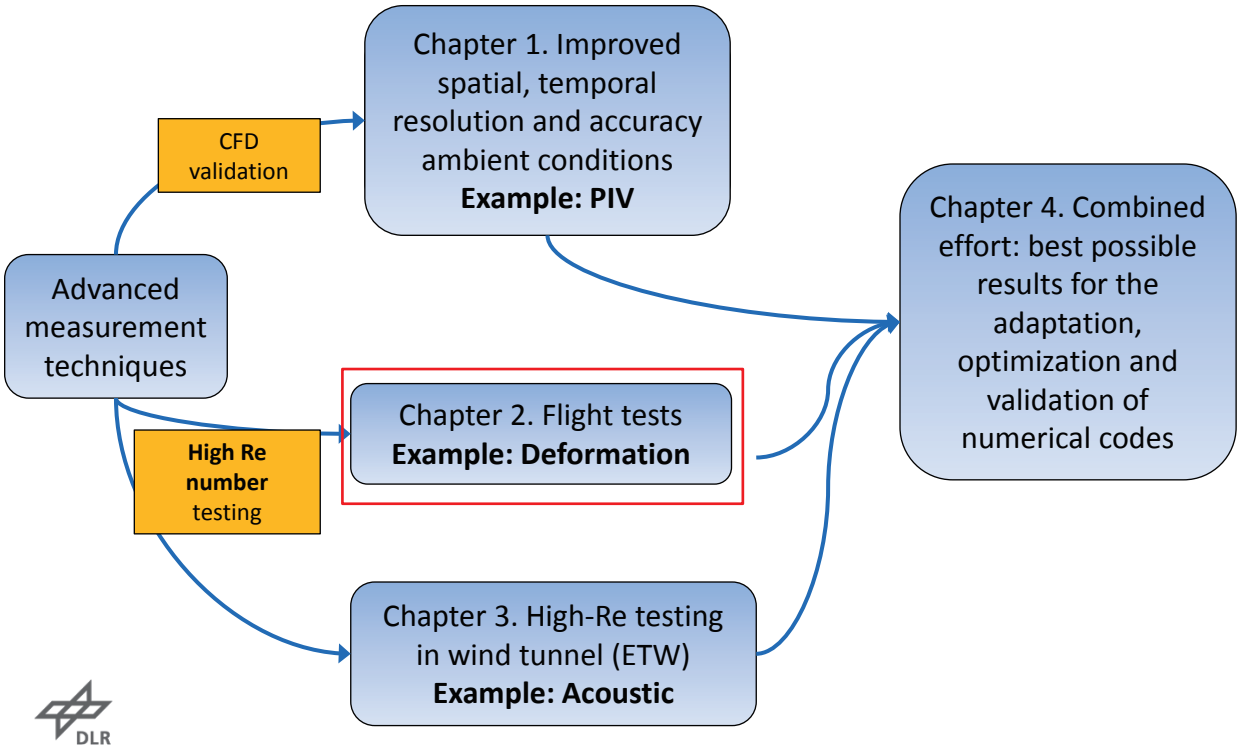


DLR

# High Reynolds number measurements

## In-flight testing

- **Flight testing**
  - Necessary part of A/C certification
  - Critical and most expensive phase
  - Provide final validation of full scale A/C design

  } Real-flight Reynolds-number
- **Advanced non-intrusive optical measurement techniques**
  - Can minimize the installation effort on the flight test bed
  - Structure has not to be modified/damaged
  - Deliver planar or volumetric measurement data
  - Well established for wind-tunnel applications
- **But they have to be:**
  - Further tested for in-flight application
  - Improved concerning user-friendliness

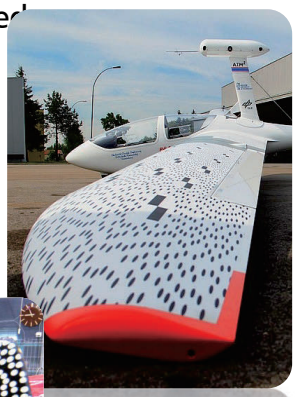

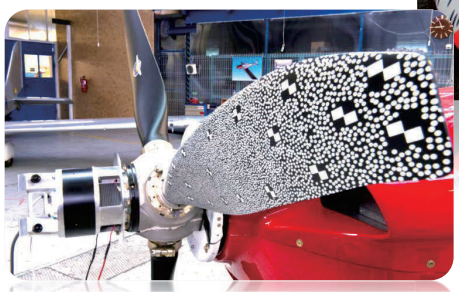



# AIM – Project Overview (1)

- **A**dvanced **I**nflight **M**easurement Techniques
  - STReP in the 6th European Framework
  - funded by the European Commission
  - Duration: 3 Years + 6 Months (11/06 – 04/10)

AIM
Advanced In-Flight Measurement Techniques

- **Objective:**
  - Testing the **feasibility of wind tunnel proven optical measurement techniques** to in-flight application
- **11 Partnerorganisations:**
  - DLR, Airbus France, Eurocopter (D+F), Piaggio, EVEKTOR, NLR, ONERA, Cranfield University, MPEI (TU),Braunschweig Airport

## AIM – Project Overview (2)

Wing deformation measurements

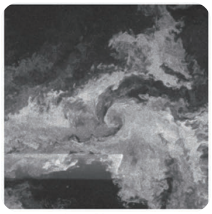

Blade tip vortex measurements

Full scale and inflight flow field investigations

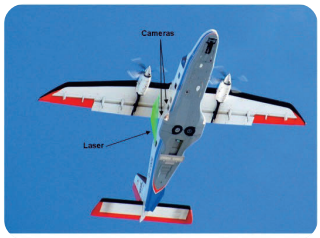


Propeller and rotor deformation measurements

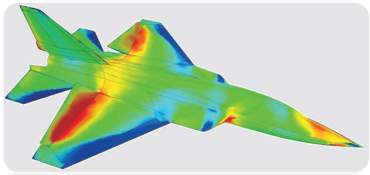

Surface pressure measurements

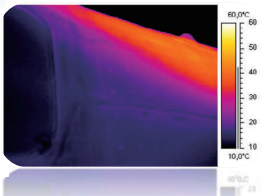

Surface temperature measurements

DLR



## AIM2 – Project Overview (1)

- **A**dvanced **I**nflight **M**easurement Techniques **2**
  - CP in the 7th European Framework
  - Duration: 42 Months + 6 Months (10/10 – 9/14)
  - Funded by the European Commission
- **Objective:**
  - **further develop of selected (AIM) optical measurement techniques** to
    - obtain **quantitative aerodynamic data**
    - be **easily and routinely applied to in-flight testing** with industrial demands
  - developing reliable and easy to use dedicated measurement systems
  - defining design and application rules for these new in-flight measurement techniques
- **11 Partnerorganisations:**
  - DLR, Airbus Operations SAS, Avia Propellers, Piaggio Aero Industries, EVEKTOR, NLR, Rzeszów University of Technology, ONERA, Cranfield University, MPEI (TU)

AIM2
Advanced In-Flight Measurement Techniques 2

DLR

## AIM² Tasks

Advanced In-Flight Measurement Techniques 2

Wing Deformation Measurements
*(IPCT)*

Propeller Deformation Measurements
*(IPCT)*

Inflight Flow Field Measurements
*(PIV)*

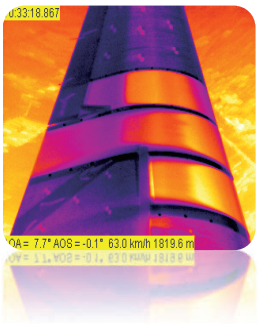

Flow Transition Measurements
*(IRT)*

Pressure and Strain Measurements
*(Fiberoptic Sensors)*

DLR

DLR.de • Chart 40 > L. Koop • High-Re Testing > July 7th 2016

## AIM2 Tasks – Example 2: Deformation

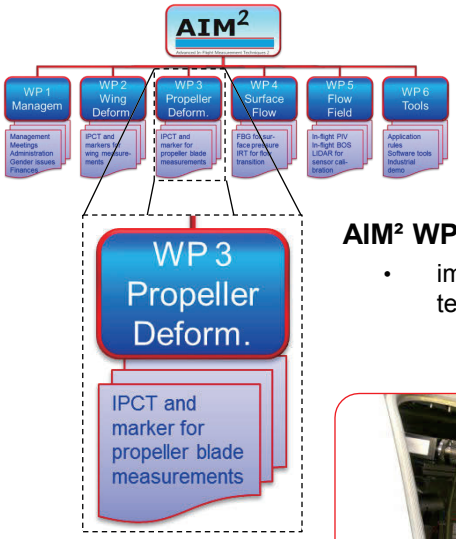


**AIM² WP 3 – Deformation Measurements on Propeller Blades**

- improvement of IPCT and Marker based deformation measurement techniques for 360° propeller deformation measurements

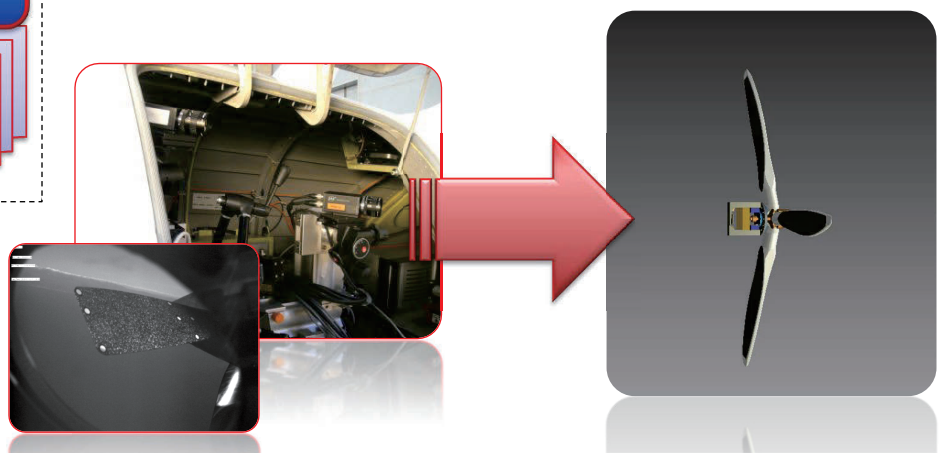

DLR

DLR.de • Chart 41 > L. Koop • High-Re Testing > July 7th 2016

## Rotating IPCT Camera System

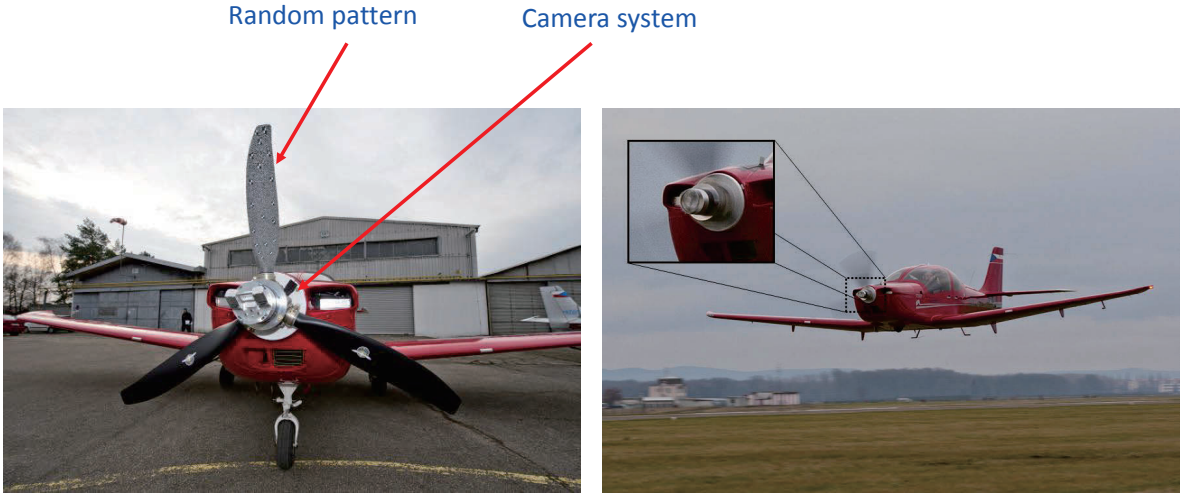


Ground test Flight test

An **IPCT measurement system is rotating together with the propeller** at its full speed.
The **blade deformation can be investigated over a complete revolution**.
A small aircraft **COBRA VUT100** has been chosen for the tests as a “worst case” because of its very high propeller rotation speed of 2700 rpm and a high vibrations of up to 20g in the range 20-150 Hz

DLR

DLR.de • Chart 42 > L. Koop • High-Re Testing > July 7th 2016

## Rotating IPCT Camera System – Detail

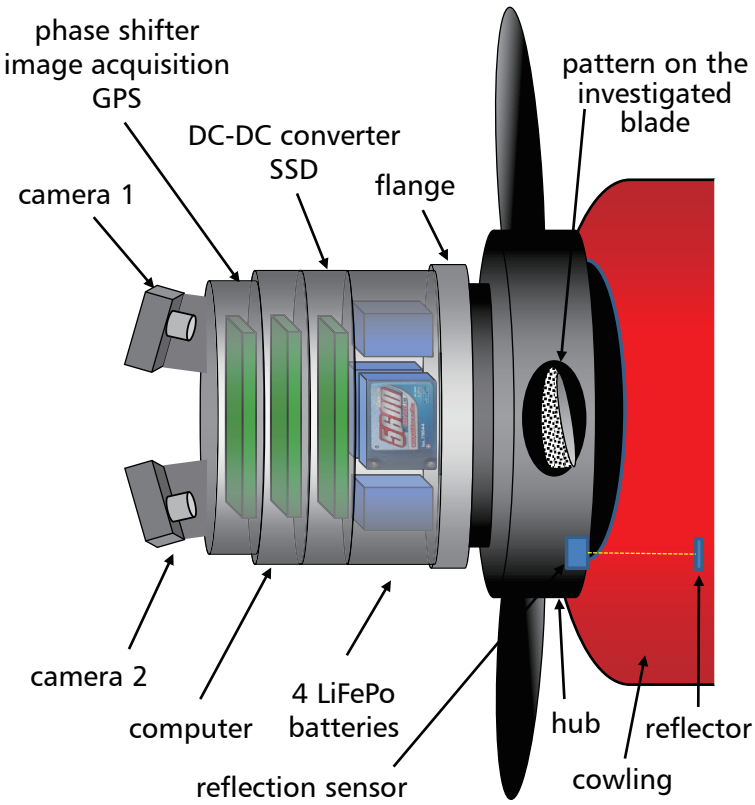


DLR

DLR.de • Chart 43 > L. Koop • High-Re Testing > July 7th 2016

## Assembling of the Rotating Camera System

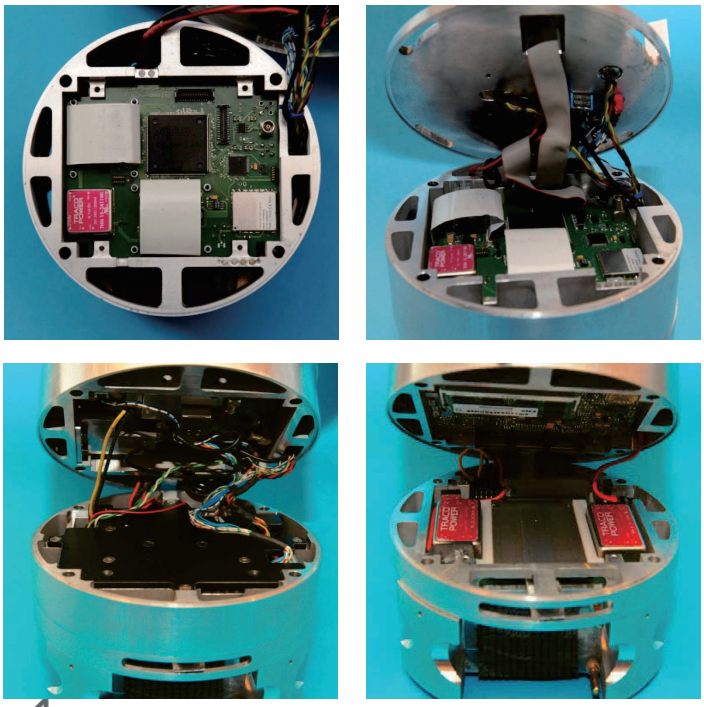

Electronic boards
of the camera system placed
inside of the cabinet

DLR

DLR.de • Chart 44 > L. Koop • High-Re Testing > July 7th 2016

## Performing the Ground Test

Calibrating procedure


Testing the WLAN connection

The aircraft ready for the ground test

The full speed ground test

## Performing the Flight Test

Ready for take-off

Take off for the flight test

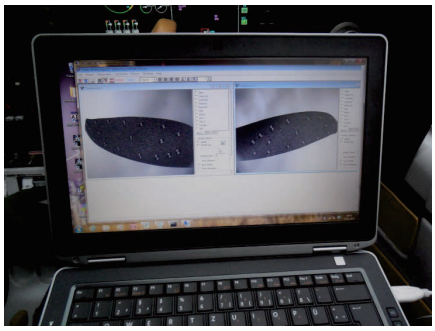

Satisfactory result
viewed on the cabin laptop

Happy team



## Example Recordings at Rotating Phase Angle


- pattern is imaged in sufficient quality (no blurring, good contrast and sharpness, size contribution uniformly)
- camera is able to cope with changing illumination (no artificial illumination required)

## Example Results

example of data extraction from several single evaluated image pairs

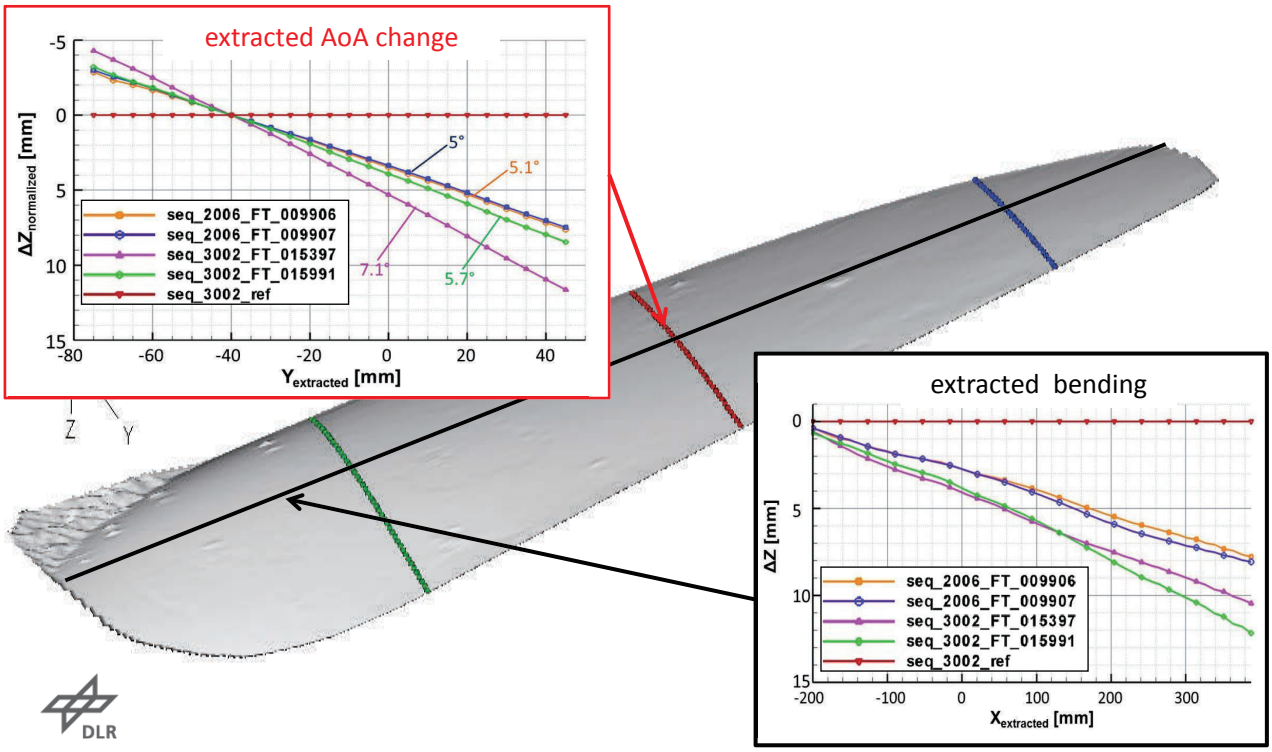




## Conclusion and Summary; Chapter 2

- Test of rotating camera performed successfully
- Feasibility of **360° propeller blade deformation measurements** with IPCT shown
- Preparation of future applications, e.g. **helicopter rotor**
- Invited lecture at the *International Congress on High-speed Imaging and Photonics*

- AIM and AIM² have been **first steps in establishing modern optical measurement techniques** in flight testing
- Important strategic development towards **high Re measurement capabilities**
- Real flight Re number measurements **requested by industry and research**

DLR.de • Chart 49 > L. Koop • High-Re Testing > July 7th 2016

## Introduction 2/2: Overview

High Re-number testing and CFD validation

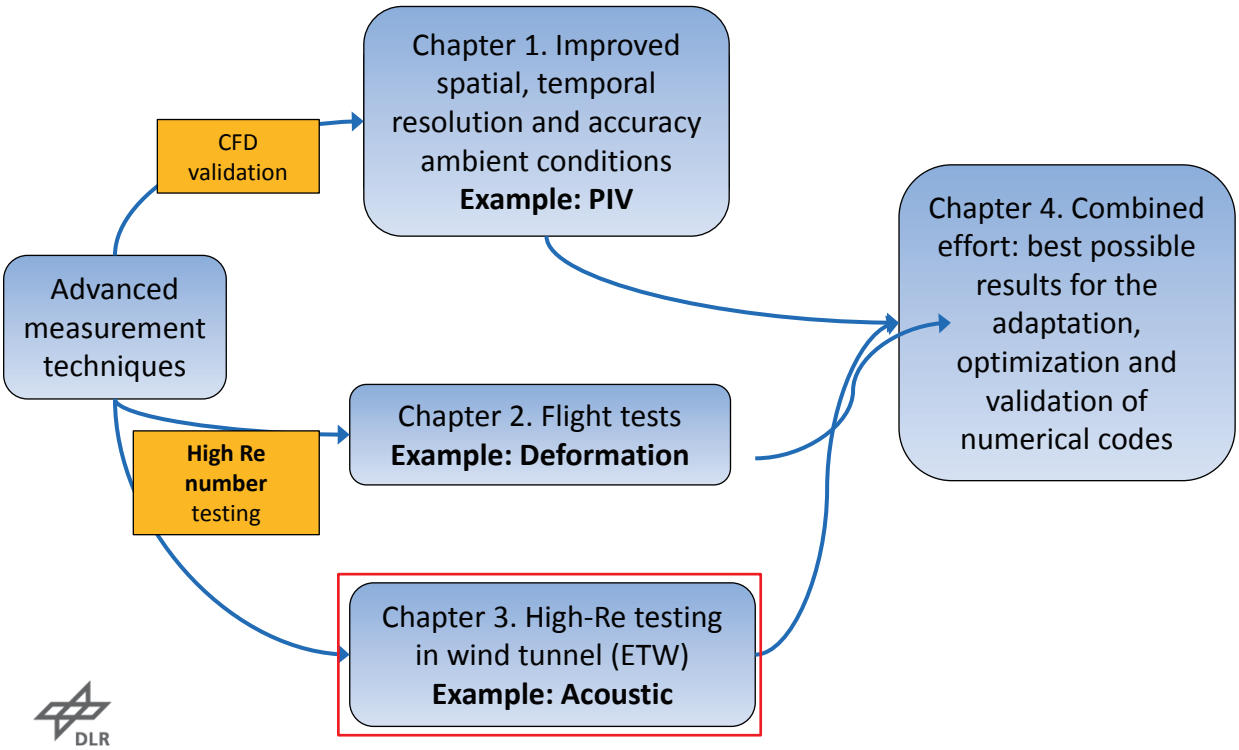


DLR

DLR.de • Chart 50 > L. Koop • High-Re Testing > July 7th 2016

## High Reynolds number measurements

European Transonic Wind tunnel (ETW)

- Common practice: Acoustic measurement on small-scale models …
- Conventional wind tunnel: real-flight Reynolds numbers not achieved
  → cryogenic and/or pressurized wind tunnel

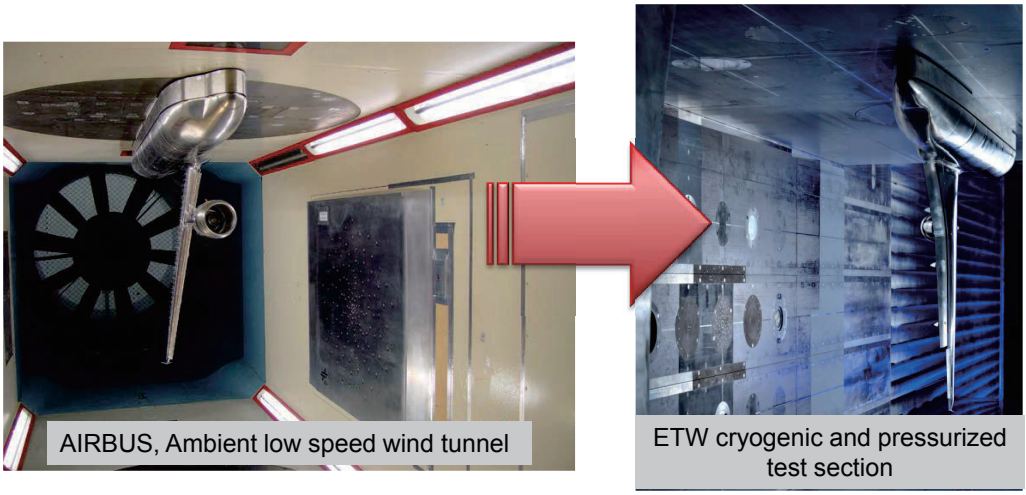


DLR

# High Reynolds number measurements

## Wind Tunnel

- European Transonic Windtunnel (ETW)
- Provision of real-flight Reynolds numbers by virtue of both decreased temperature and increased pressure
- Test section:
  2.0 m x 2.4 m x 9.0 m
- Operational range:

| |
|---|
| **0.15 < *M* < 1.35** |
| 313 K > *T* > 110 K |
| 110 kPa < $p_{tot}$ < 450 kPa |

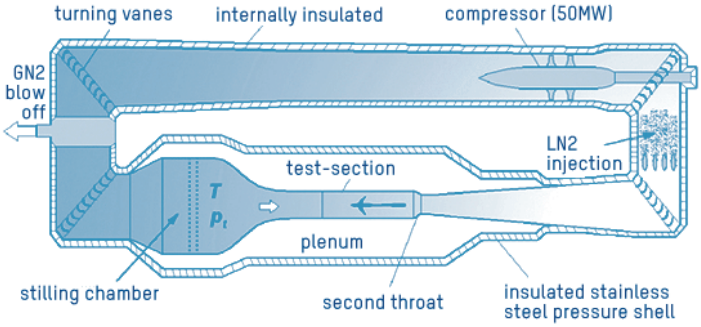






# High Reynolds number measurements in ETW

## Cryogenic & pressurized *Microphones*

Brüel&Kjær cryogenic-type 4944A

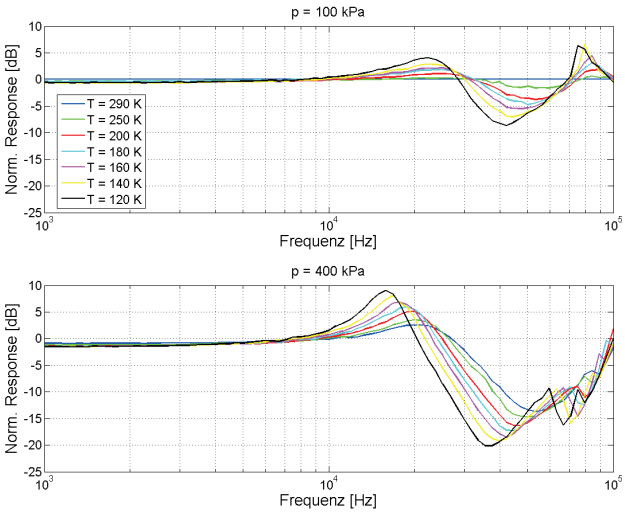


- Variation of amplitude response:
  ⇨ function of *T* and $p_{tot}$
  (known from manufacturer and a previous test*)

Ahlefeldt T. et. al., "High-Reynolds Number Aeroacoustic Testing under Pressurized Cryogenic Conditions in PETW", *50th AIAA-ASM*, 2012.

# High Reynolds number measurements in ETW

## Array optimization

Microphone-Array

- 96 microphones (flush mounted)
- Inserts: compressed laminated wood

Brüel&Kjær cryogenic-type 4944A

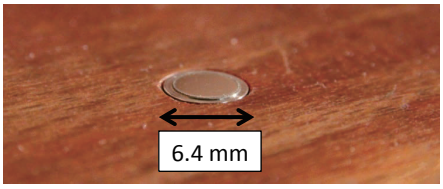


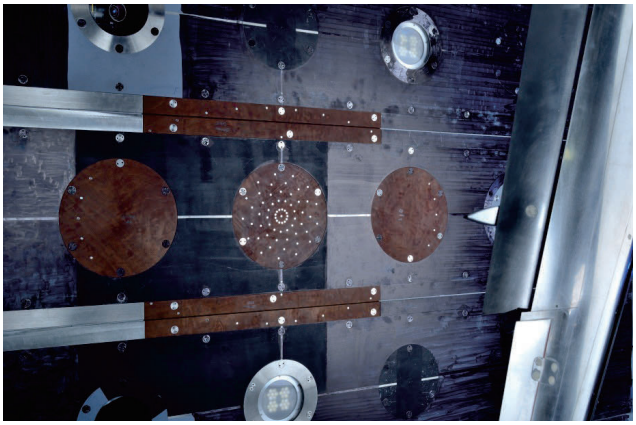



# High Reynolds number measurements in ETW

## Array pattern

- Limited positioning of microphones:
  - Significantly restricted angle/area of observation
  - Conventional BF-maps: strong sidelobes

- Different microphone groups used for conventional maps ("nested arrays")

- All microphones used for CLEAN-SC maps

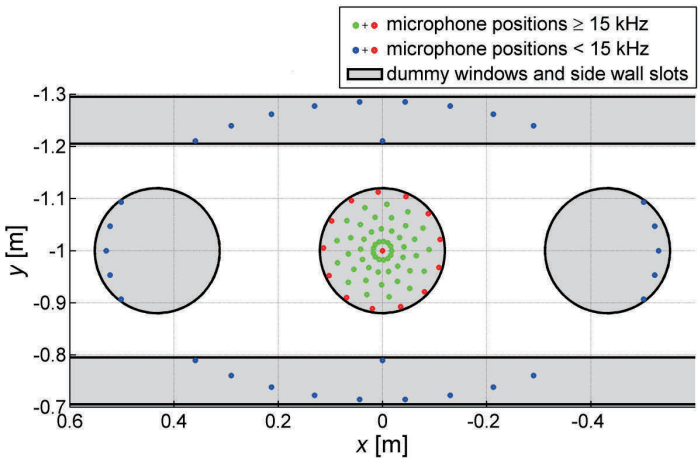

# High Reynolds number measurements in ETW

## Setup

Airbus K3DY half-model

- Scale: 1:13.6 (7.35%)
- High-lift configuration identical to EWA-Benchmark test 2007 at LSWT

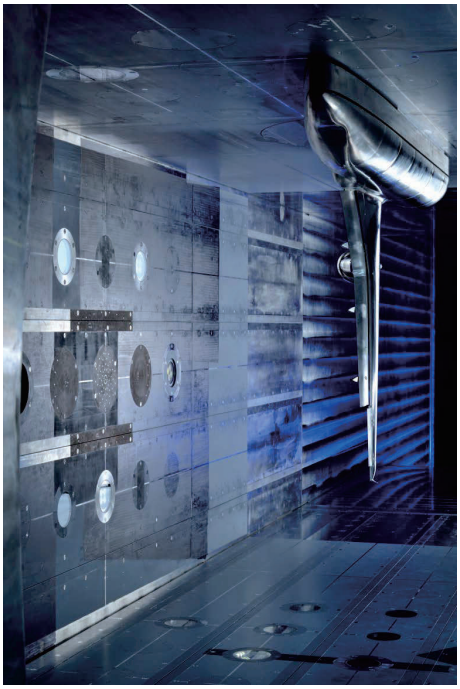

Data points ($M$ = 0.203)

| | $T$ [K] | $p_{tot}$ [kPa] | $Re_\delta$ [$10^6$] | $q/E$ [$10^{-8}$] |
|---|---|---|---|---|
| DP I | 310 | 110 | 1.42 | 1.57 |
| DP II | 125 | 115 | 5.16 | 1.57 |
| DP III | 310 | 399 | 5.16 | 5.70 |
| DP IV | 120 | 419 | 20.00 | 5.70 |



# Results – Source maps (CLEAN-SC)

M = *0.203* | *α = 3°* / *Variation of Strouhal number*

- Different Reynolds number
- **7%** to **26%** of real-flight $Re_\delta$
- Same deformation

| $Re_\delta = 1.42 \cdot 10^6$ |
|---|
| $q/E = 1.57 \cdot 10^{-8}$ |

| $Re_\delta = 5.16 \cdot 10^6$ |
|---|
| $q/E = 1.57 \cdot 10^{-8}$ |

# Results – Source maps (CLEAN-SC)

M = *0.203* | *α = 3°* / *Variation of Strouhal number*

**$St_{\delta,1/3Oct}$ = 20**

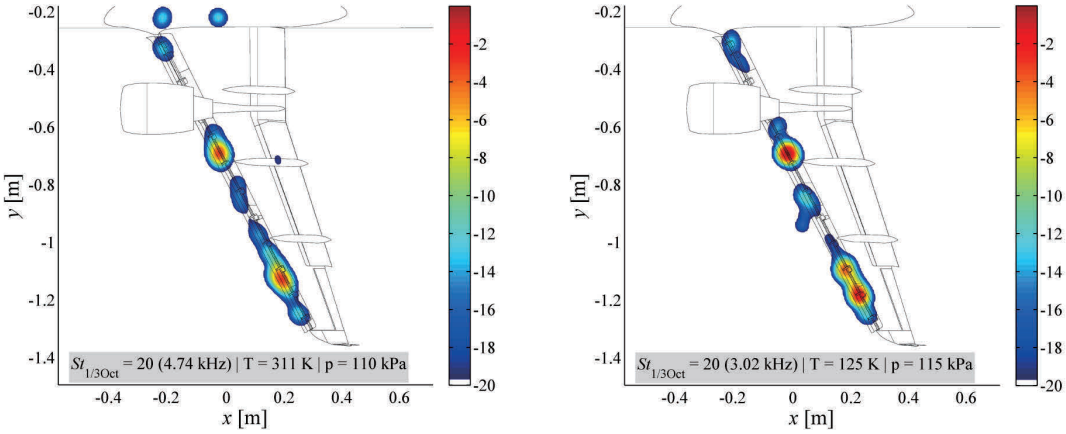


| | |
|---|---|
| **$Re_\delta$ = 1.42·10$^6$** | **$Re_\delta$ = 5.16·10$^6$** |
| $q/E$ = 1.57·10$^{-8}$ | $q/E$ = 1.57·10$^{-8}$ |



# Results – Source maps (CLEAN-SC)

M = *0.203* | *α = 3°* / *Variation of Strouhal number*

**$St_{\delta,1/3Oct}$ = 130**

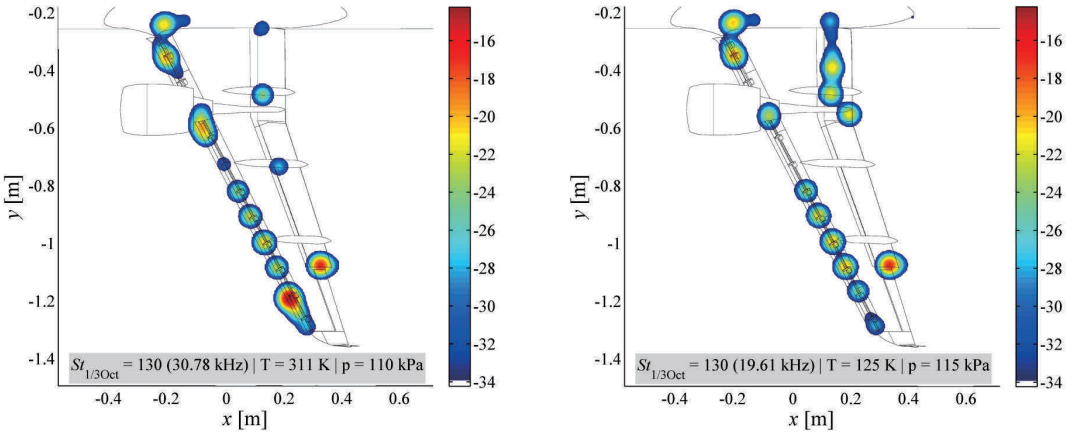


| | |
|---|---|
| **$Re_\delta$ = 1.42·10$^6$** | **$Re_\delta$ = 5.16·10$^6$** |
| $q/E$ = 1.57·10$^{-8}$ | $q/E$ = 1.57·10$^{-8}$ |

## Results – Source maps (CLEAN-SC)

M = *0.203* | *α = 3°* / *Variation of Strouhal number*

**$St_{\delta,1/3Oct}$ = 200**

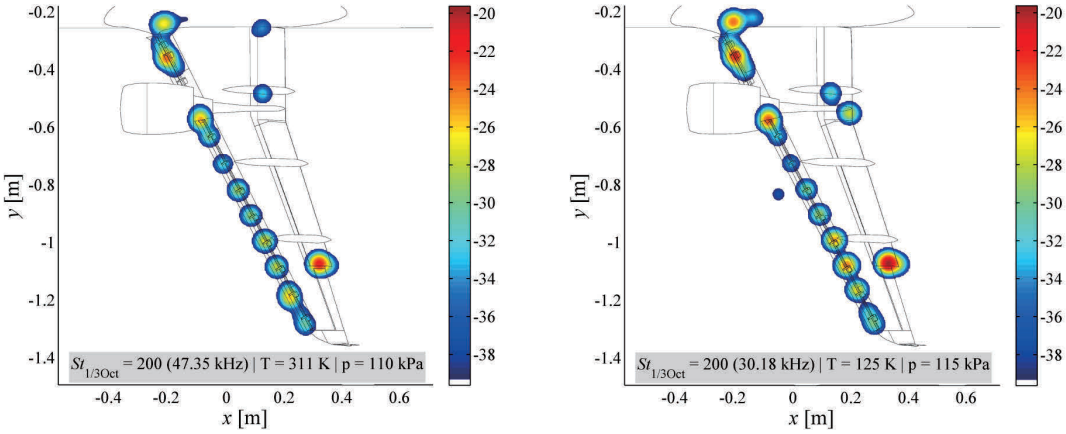


| | |
|---|---|
| **$Re_\delta$ = 1.42·10$^6$** | **$Re_\delta$ = 5.16·10$^6$** |
| $q/E$ = 1.57·10$^{-8}$ | $q/E$ = 1.57·10$^{-8}$ |



## Results – Source maps (CLEAN-SC)

M = *0.203* | *α = 3°* / *Variation of Strouhal number*

- Different Reynolds number
- **26%** to **100%** of real-flight $Re_\delta$
- Same deformation

| | |
|---|---|
| **$Re_\delta$ = 5.16·10$^6$** | **$Re_\delta$ = 20.0·10$^6$** |
| $q/E$ = 5.70·10$^{-8}$ | $q/E$ = 5.70·10$^{-8}$ |

# Results – Source maps (CLEAN-SC)

M = *0.203* | *α = 3°* / *Variation of Strouhal number*

**$St_{\delta,1/3Oct}$ = 20**

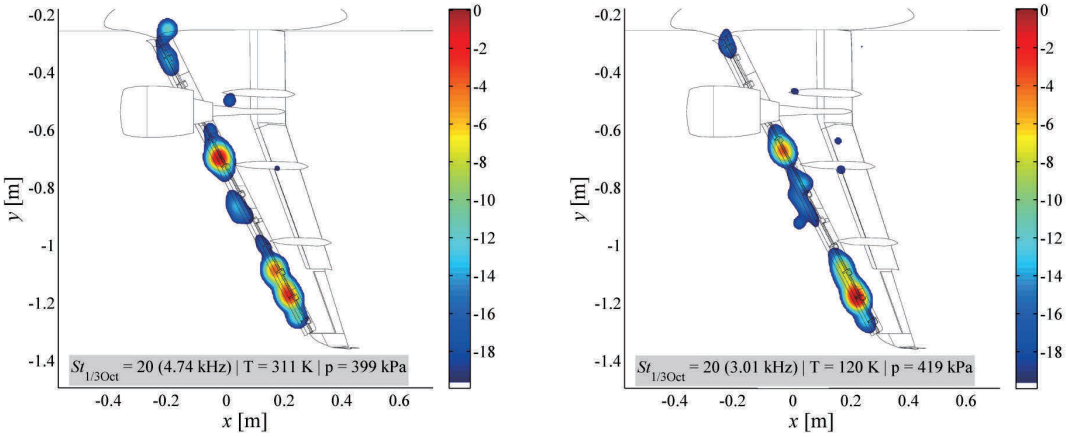


| | |
|---|---|
| $Re_\delta = 5.16 \cdot 10^6$ | $Re_\delta = 20.00 \cdot 10^6$ |
| $q/E = 5.70 \cdot 10^{-8}$ | $q/E = 5.70 \cdot 10^{-8}$ |



# Results – Source maps (CLEAN-SC)

M = *0.203* | *α = 3°* / *Variation of Strouhal number*

**$St_{\delta,1/3Oct}$ = 130**

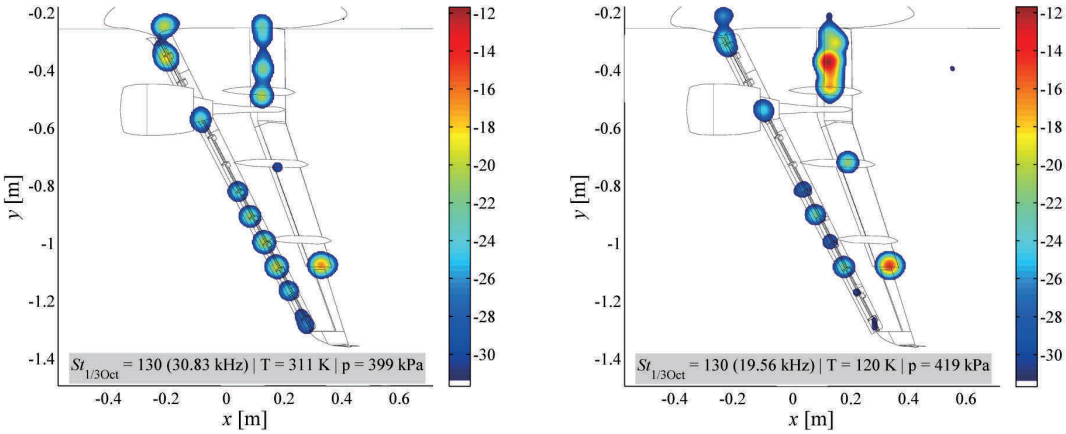


| | |
|---|---|
| $Re_\delta = 5.16 \cdot 10^6$ | $Re_\delta = 20.00 \cdot 10^6$ |
| $q/E = 5.70 \cdot 10^{-8}$ | $q/E = 5.70 \cdot 10^{-8}$ |

# Results – Source maps (CLEAN-SC)

M = *0.203* | *α = 3°* / *Variation of Strouhal number*

**$St_{\delta,1/3Oct}$ = 200**

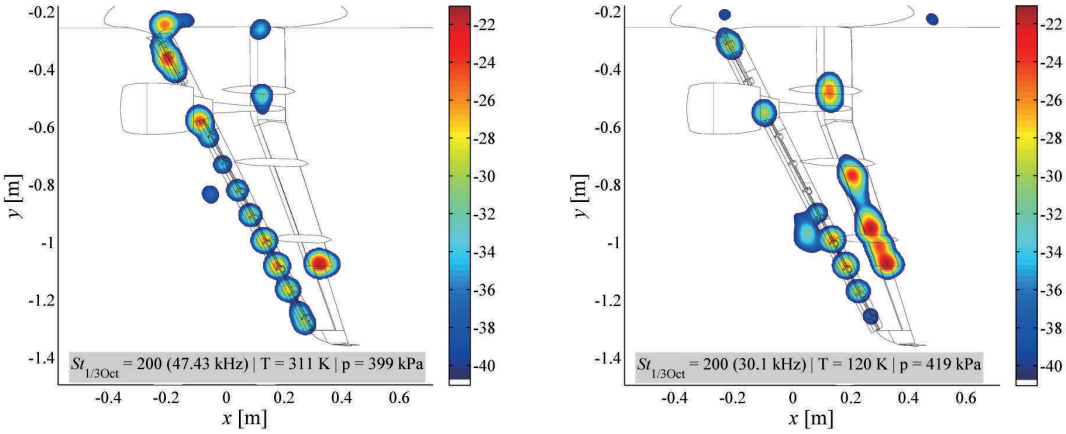


| | |
|---|---|
| $Re_\delta = 5.16 \cdot 10^6$ | $Re_\delta = 20.00 \cdot 10^6$ |
| $q/E = 5.70 \cdot 10^{-8}$ | $q/E = 5.70 \cdot 10^{-8}$ |



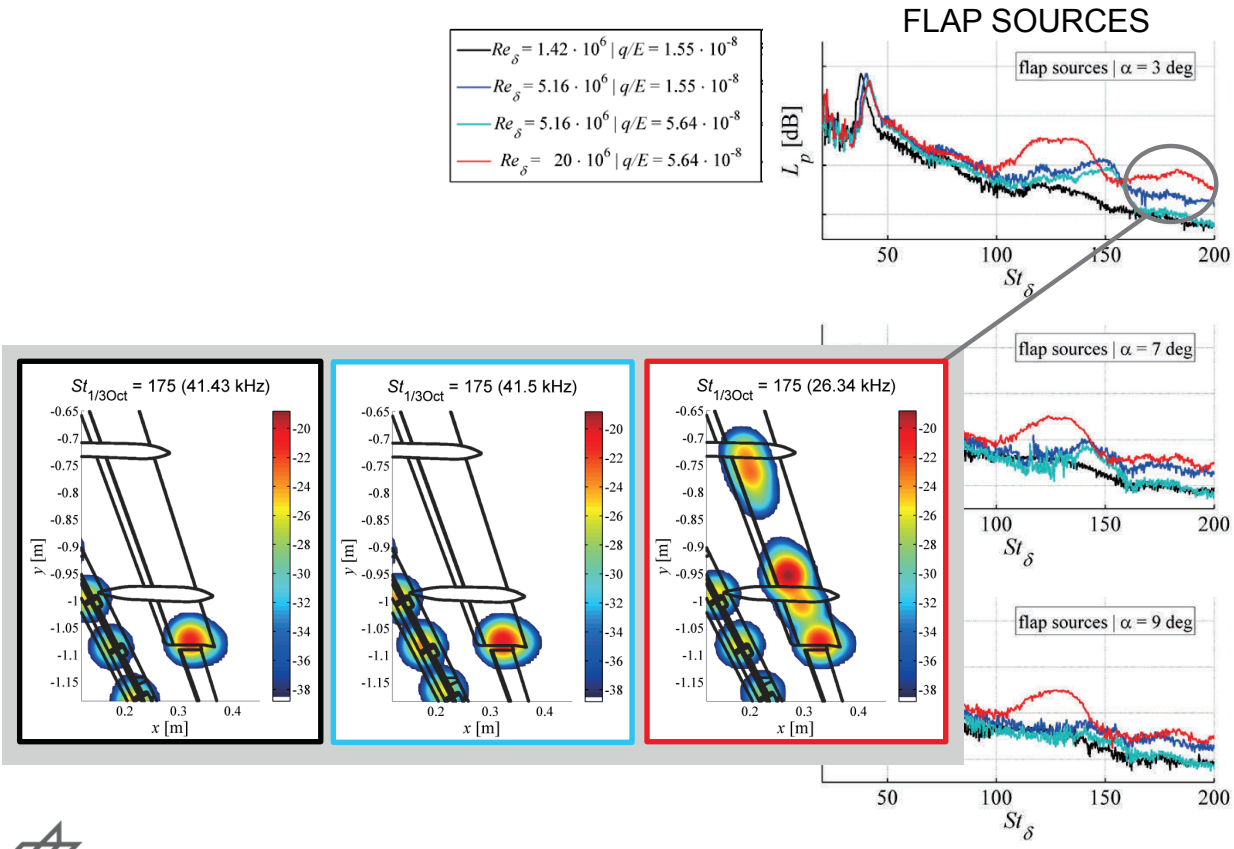

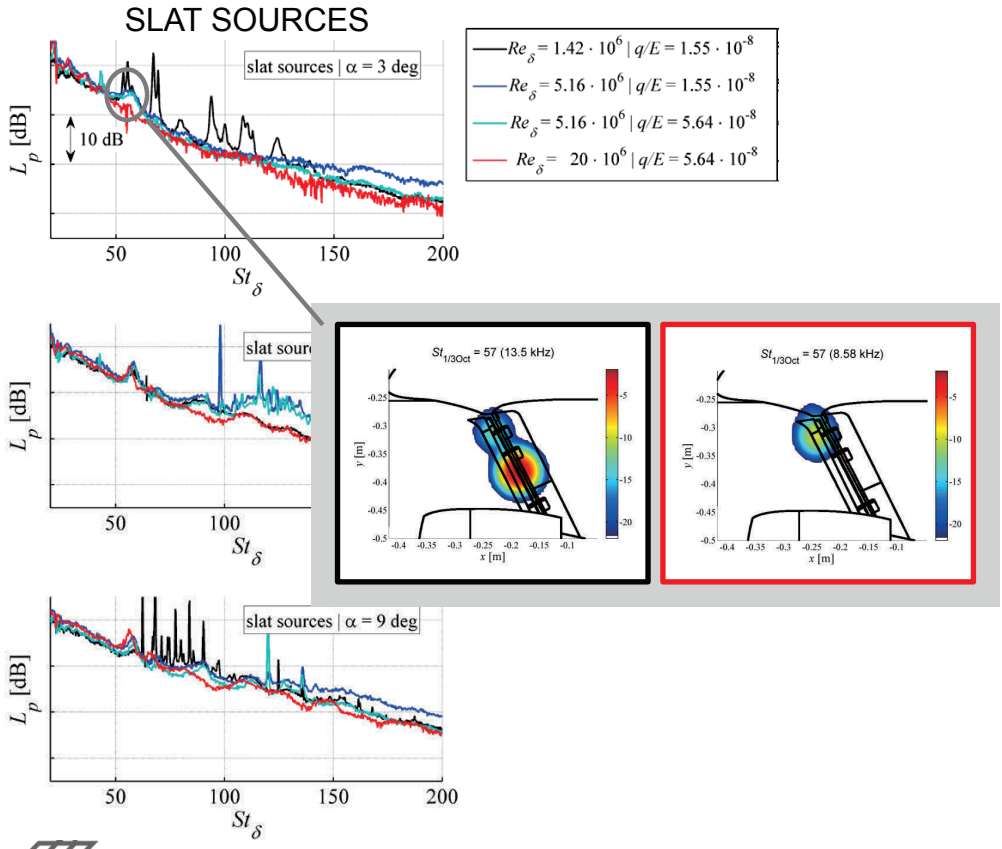




# Summary; Chapter 3

- First time: airframe noise data of a small-scale model at real-flight Reynolds numbers
- Significant Reynolds number dependency
  - $St_\delta$ < 100 ($f_{original}$ < 1,8 kHz):
    - Slat tones at low *Re*
    - Various peaks with combined *Re* & *St* dependency
  - $St_\delta$ > 100 ($f_{original}$ > 1,8 kHz):
    - Inboard slat sources at mid-level *Re*
    - Dominant broadband peaks on flap at real-flight *Re*
      - ! flap more dominant than slat !

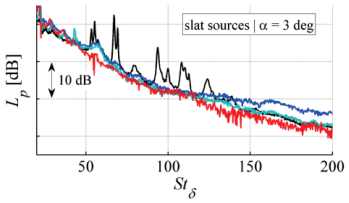


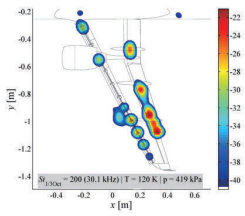

# Advanced measurement techniques in ETW

## Operational techniques

| TSP | PIV | Sound pressure | PSP |
|---|---|---|---|
| 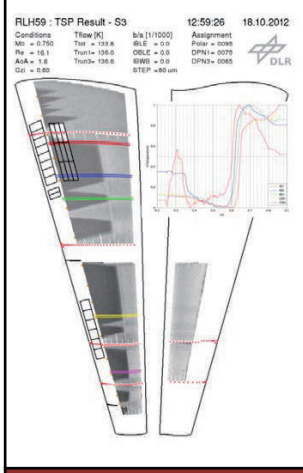 | 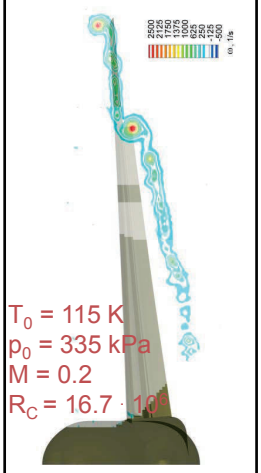  | 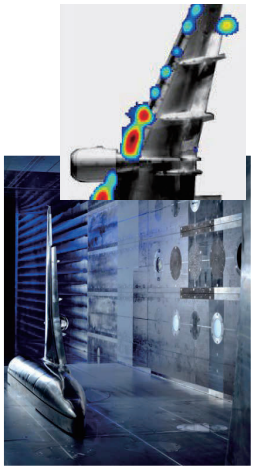 | 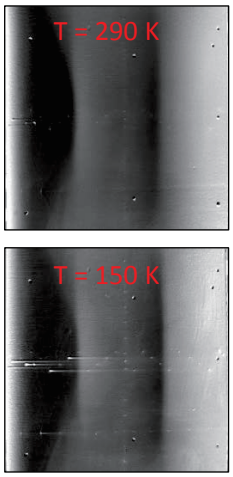  |
| Mature | Mature | Mature | Current development |



# Introduction 2/2: Overview

## High Re-number testing and CFD validation

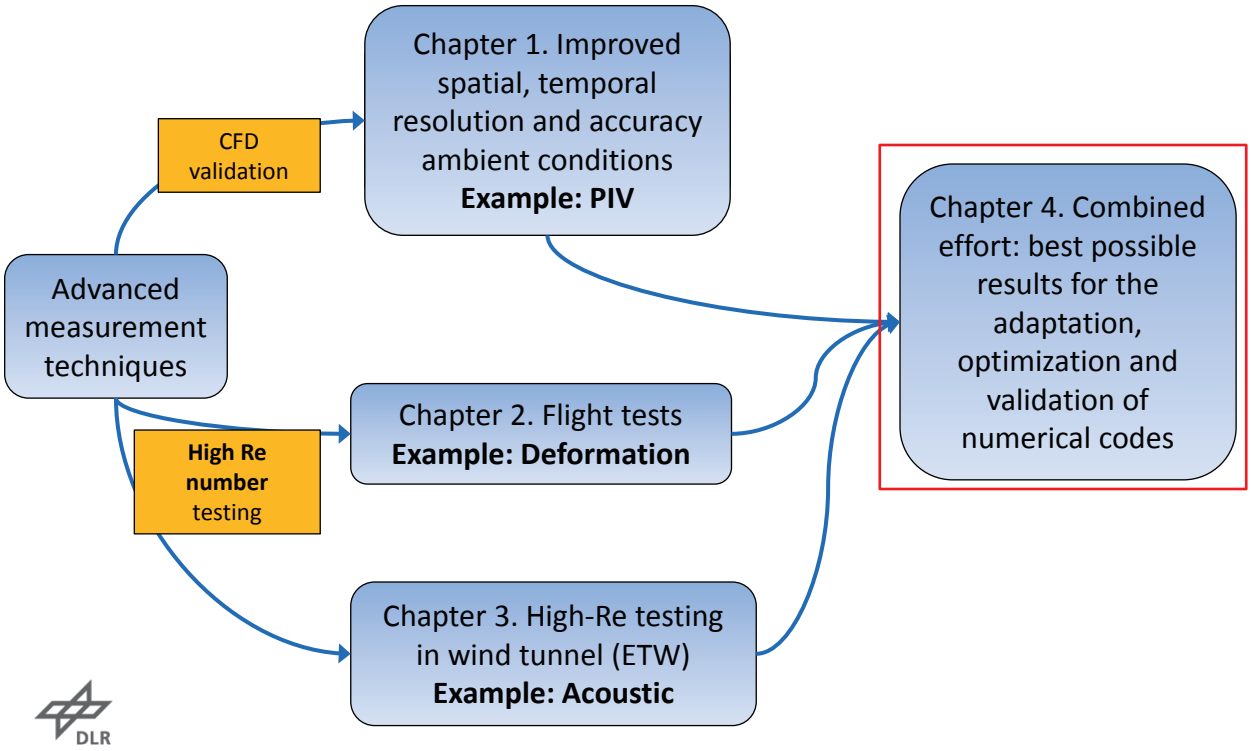

DLR.de • Chart 69 > L. Koop • High-Re Testing > July 7th 2016

# High-Lift In-Flight Validation („HINVA“)

## Basic idea

- High lift performance is an essential design parameter of transport aircrafts
- Maximum lift predictions are still characterized by considerable deviations from final performance flight test results
- Provide data base at maximum lift through wind tunnel and flight tests
- Synergetic benefits from all three methods

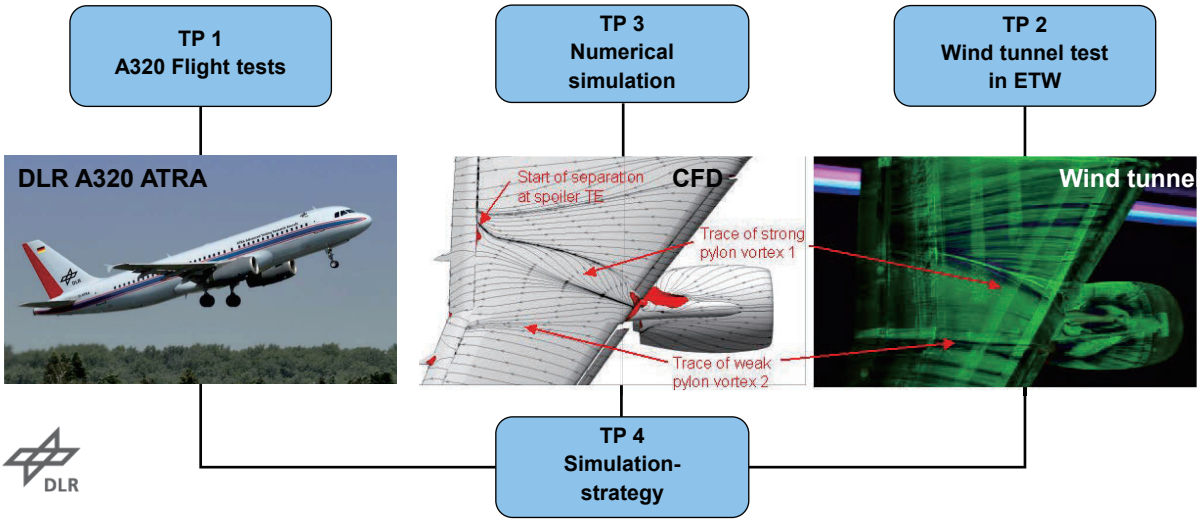


DLR.de • Chart 70 > L. Koop • High-Re Testing > July 7th 2016

# HINVA flight test #1: Overview

## DLR research aircraft ATRA (A320)

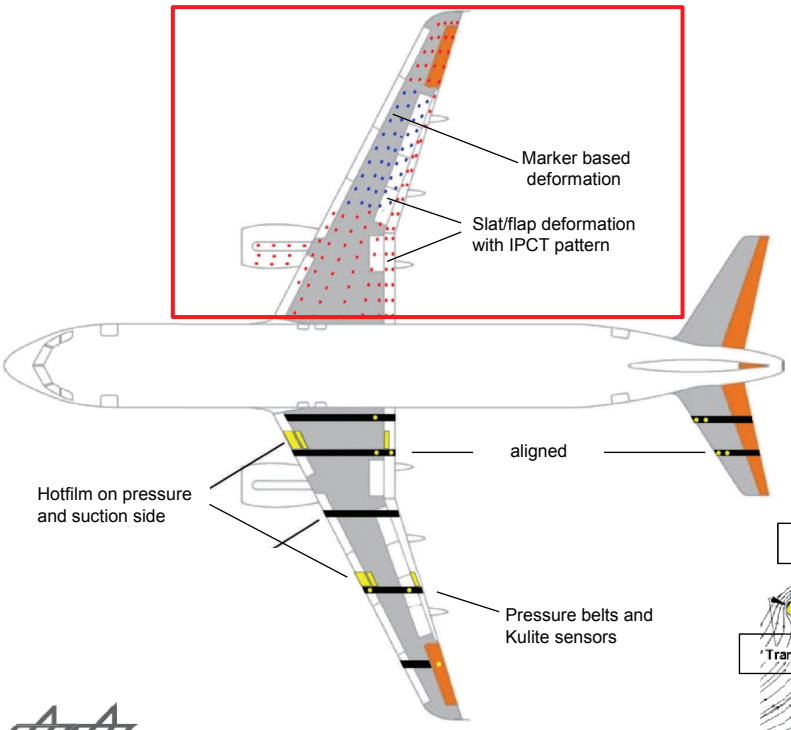


- ⇨ Deformation measurements
- ⇨ Slat/Flap gap measurements
- ⇨ Flow visualization
- ⇨ Surface pressure (probes)
- ⇨ Transition detection

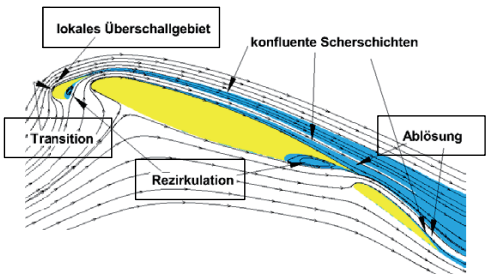


DLR DLR

# HINVA flight test #1: IPCT deformation measurement

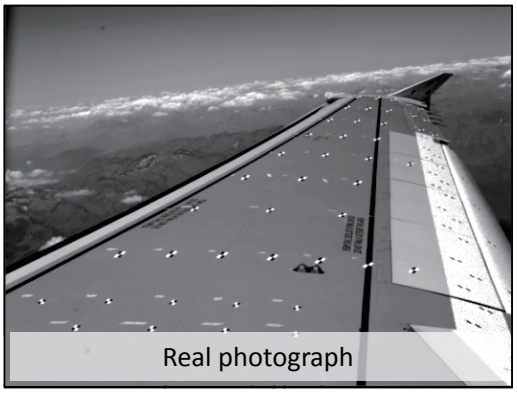


Marker technique to measure global wing deformation

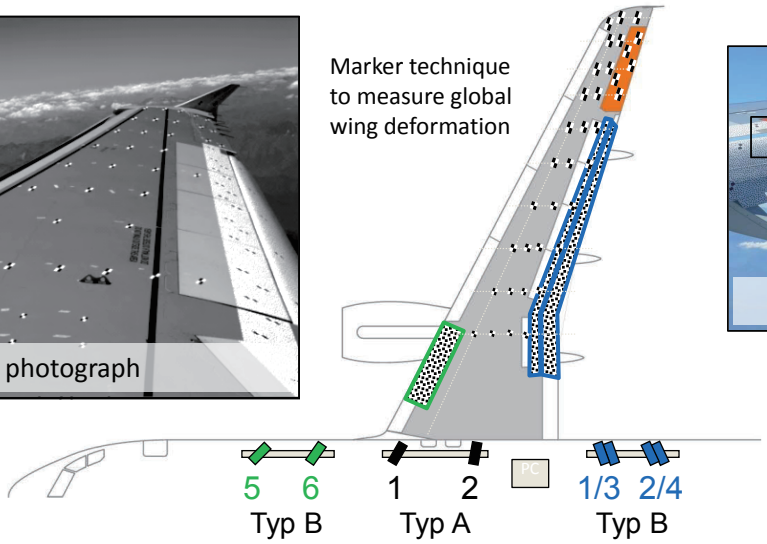


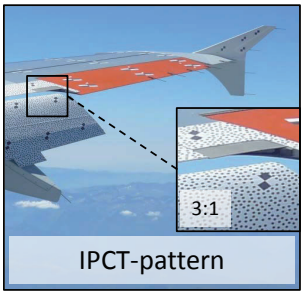


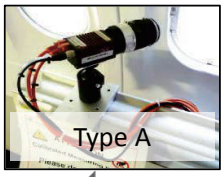


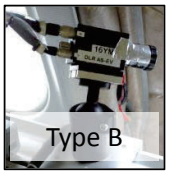



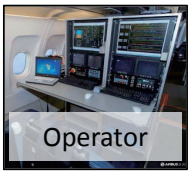


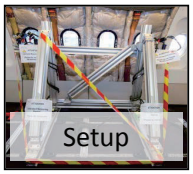


DLR



# HINVA flight test #1: Marker based deformation measurement

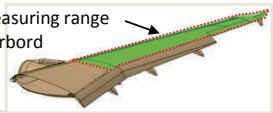


Marker based methods / global wing deformation

**Straight flight (stabilised)**

Bending and torsion (halfspan

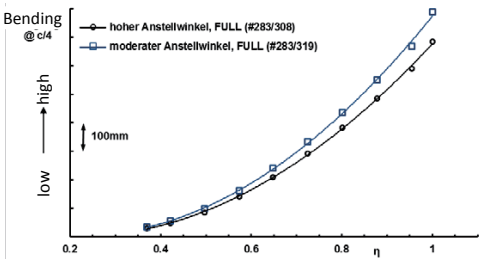


Results provide important reference data:

**Design of detailed wind tunnel model**

Verification of numerical calculations

**Dynamic stall maneuver**

Time response of bending and torsion close to wingtip

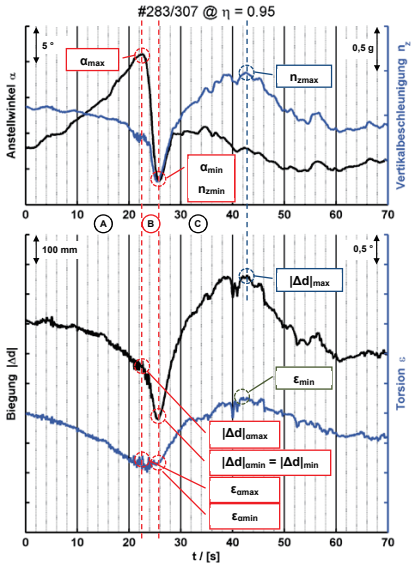


Phasen:

- (A) Increase of AoA
- (B) Stall
- (C) Stall recovery

Legende:

α ... Angle of attack
$n_z$ ... Vertical acceleration
|Δd| ... Bending (3D)
ε ... Angle of torsion
η ... normalized half span width

DLR

DLR.de • Chart 73 > L. Koop • High-Re Testing > July 7th 2016

# HINVA flight test #1: IPCT deformation measurement

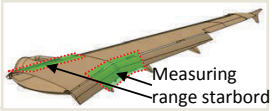


IPCT / Slat and flaps

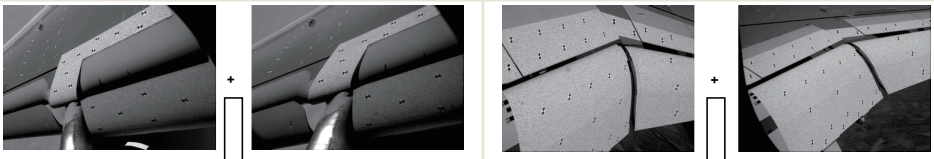

**Straight flight (stabilised)**
Backturn [°] of slat/flap

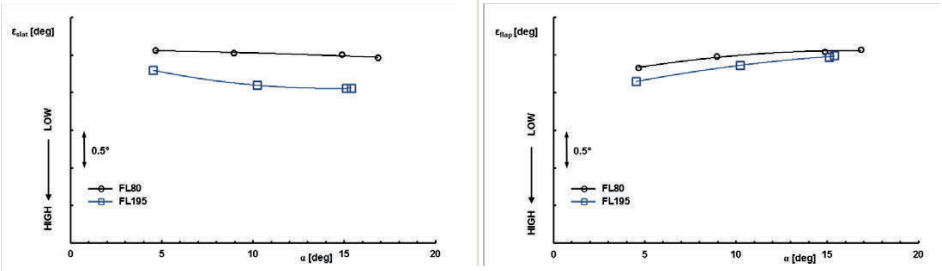


Results provide important reference data:
Investigation of **slat and flap gaps during landing approach**
Further developments of IPCT evaluation algorithm

DLR

DLR.de • Chart 74 > L. Koop • High-Re Testing > July 7th 2016

# HINVA ETW test: PIV flow field measurement

Model based on flight test #1

Reduction of background light and laser light flare on the model surfaces

- Wing, slats, fuselage and nacelle are partly coated by a PIV paint (primer + acrylic black paint)
- Polishing of paint to obtain high glossy surface finish
- Pressure taps treatment

DLR

# HINVA ETW test: PIV flow field measurement

## Stereo-PIV Arrangement

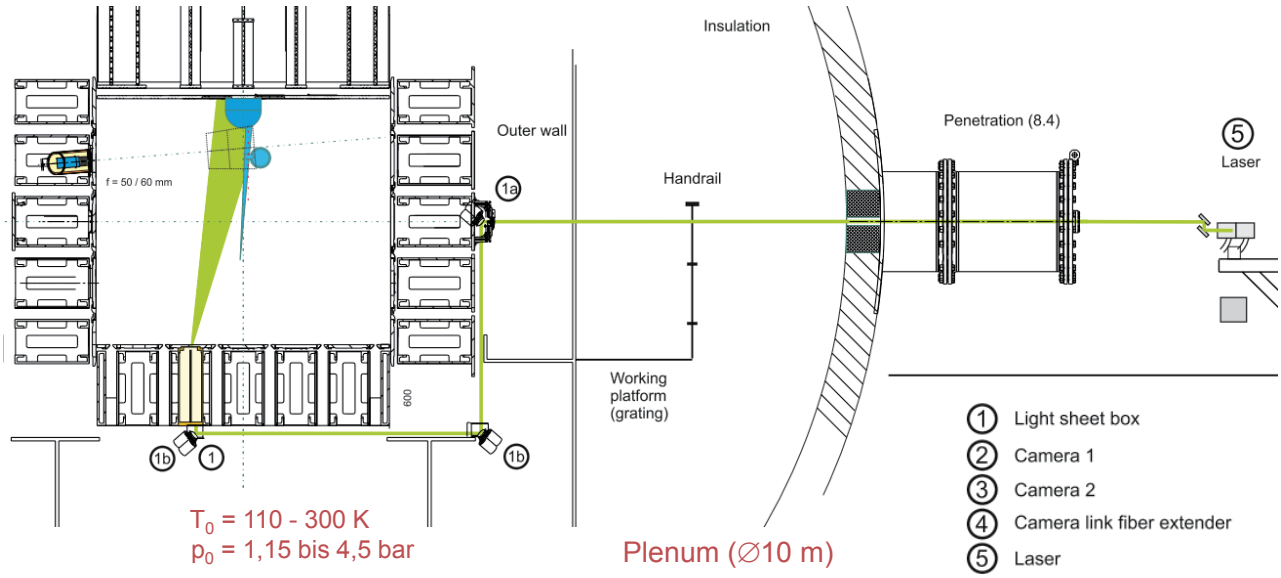






# HINVA ETW test: PIV flow field measurement

## Cryo PIV system for ETW

- Seeding system

  ⇒Generation of tiny ice particles using external DLR Laskin generators

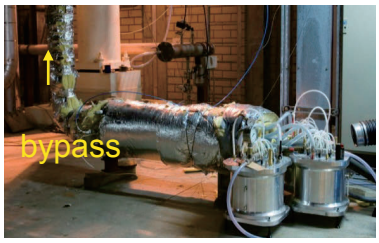


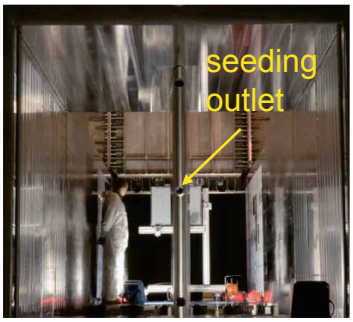


Requirements:

Flow tracer size ≅ 1 $\mu$m
Concentration of up to 10 particles / mm³

- Laser system placed outside of the wind tunnel plenum

  ⇒ Nd:YAG laser
  2 x 500 mJ @ 15 Hz

DLR.de • Chart 77 > L. Koop • High-Re Testing > July 7th 2016

## HINVA ETW test: PIV flow field measurement

Cryo PIV system for ETW

- Modules containing **cameras, light sheet optics, beam monitor** and electronics for remote control for a placement within the plenum using heated housings

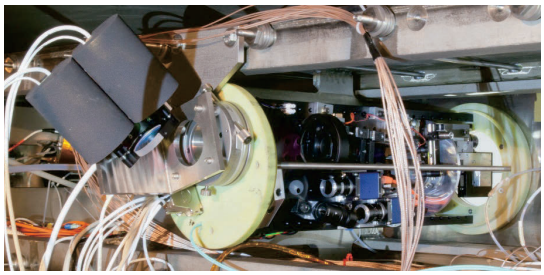

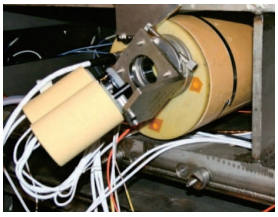

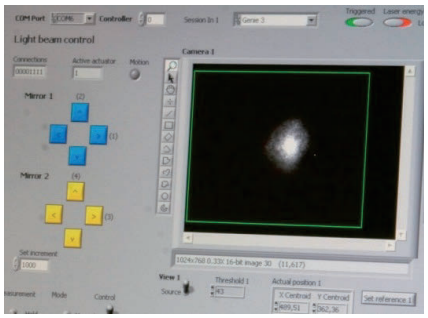


- Mirror modules
  - ⇒Equipped with piezo actuators
  - ⇒Software allows for **automatic beam path corrections** in case of beam deflections

DLR

DLR.de • Chart 78 > L. Koop • High-Re Testing > July 7th 2016

## HINVA ETW test: PIV flow field measurement

Stereo-PIV Arrangement

- Adaptation and installation of **Light Sheet Module**:
  - Motorized laser mirrors allow for a pivoting of the light sheet about three spatial axes by remote control

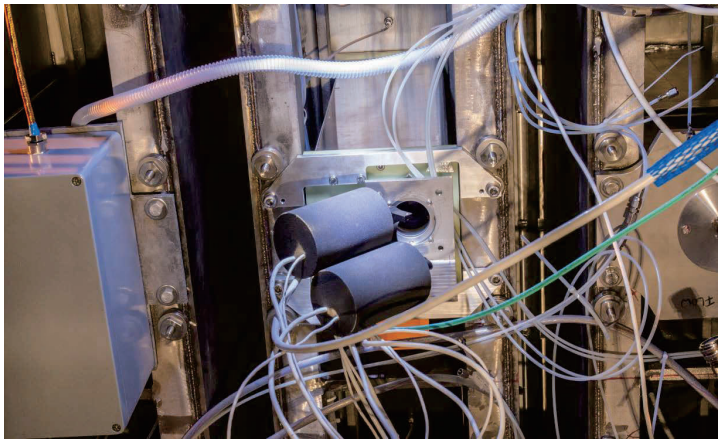

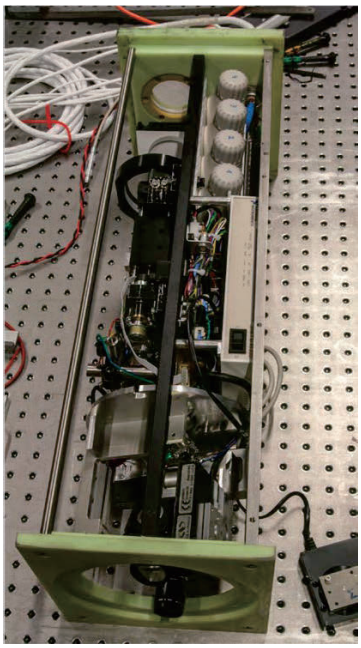

DLR

# HINVA ETW test: PIV flow field measurement

## Stereo-PIV Arrangement

- **Camera module** for viewing angles of about ±45°
  - Variable orientation of the light sheet

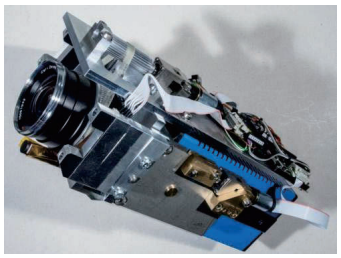

Lens focus

Scheimpflug angle

Scheimpflug axis

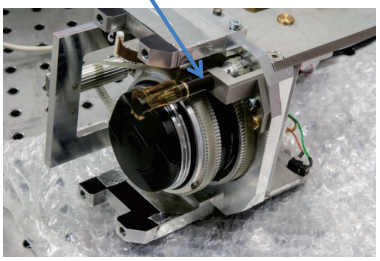

- Equipped with PCO.edge cameras,
  CMOSs sensor (2560 x 2160 px)
  direct recording to RAID
  storage system @ 15 Hz



# HINVA ETW test: PIV flow field measurement

## Vorticity distributions

Configuration 2
M = 0.186
$Re_C$ = 13.3 Mio.
α = 16.5°

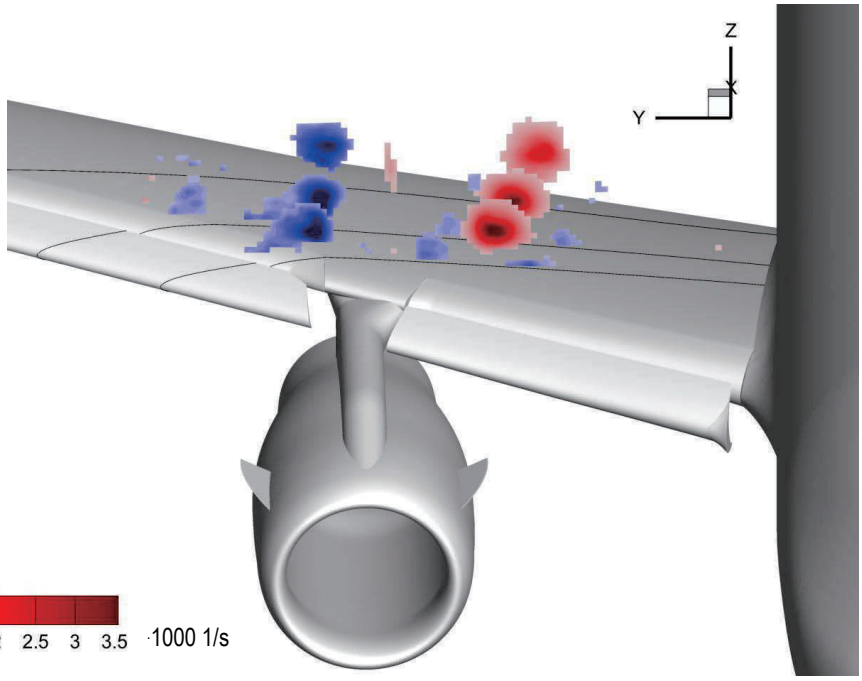

DLR.de • Chart 81 > L. Koop • High-Re Testing > July 7th 2016

# HINVA flight test #2: In-flight PIV

## PIV Configuration

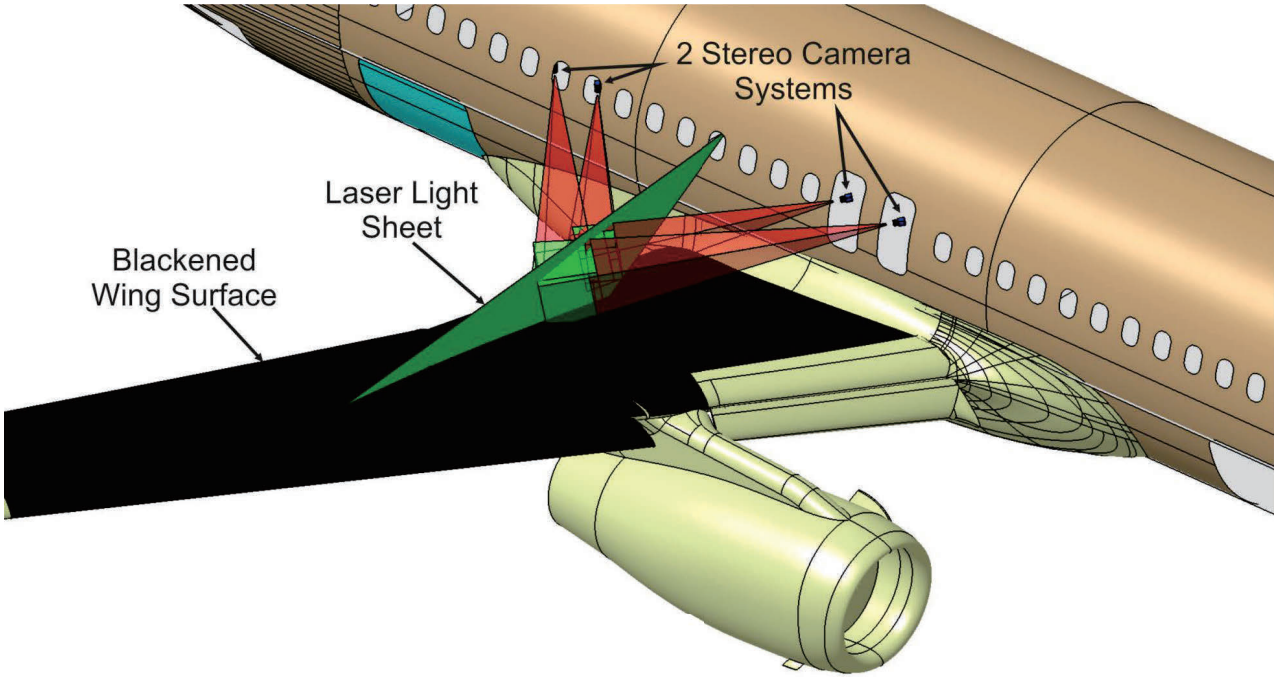


DLR

DLR.de • Chart 82 > L. Koop • High-Re Testing > July 7th 2016

# HINVA flight test #2: In-flight PIV

## Cabin Layout

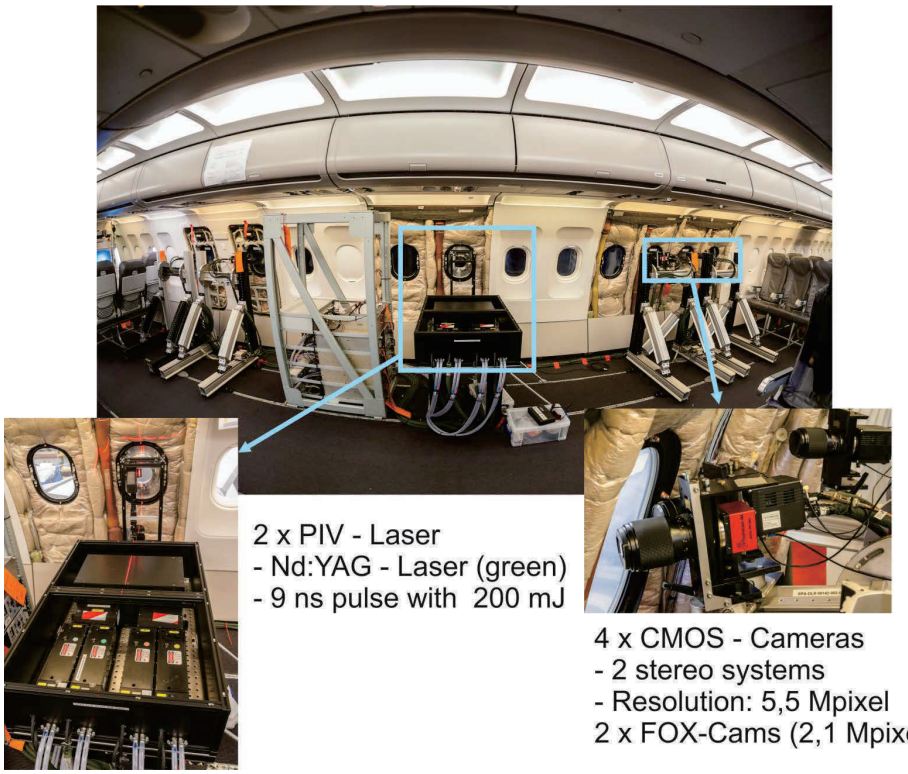


DLR

DLR.de • Chart 83 > L. Koop • High-Re Testing > July 7th 2016

## HINVA flight test #2: In-

Camera incl. Stand

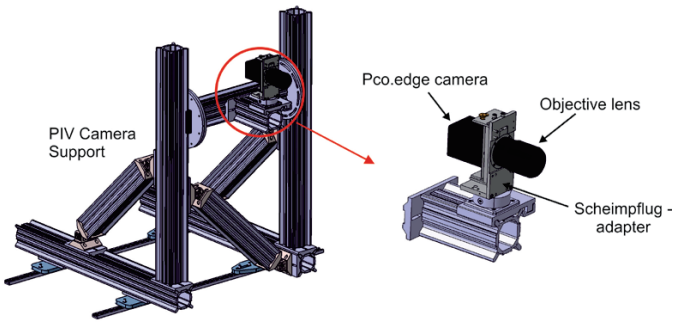


DLR.de • Chart 84 > L. Koop • High-Re Testing > July 7th 2016

## HINVA flight test #2: In-flight PIV

PIV Results: $\alpha$ = 15,6°, FL100, IAS ~ 110 kt

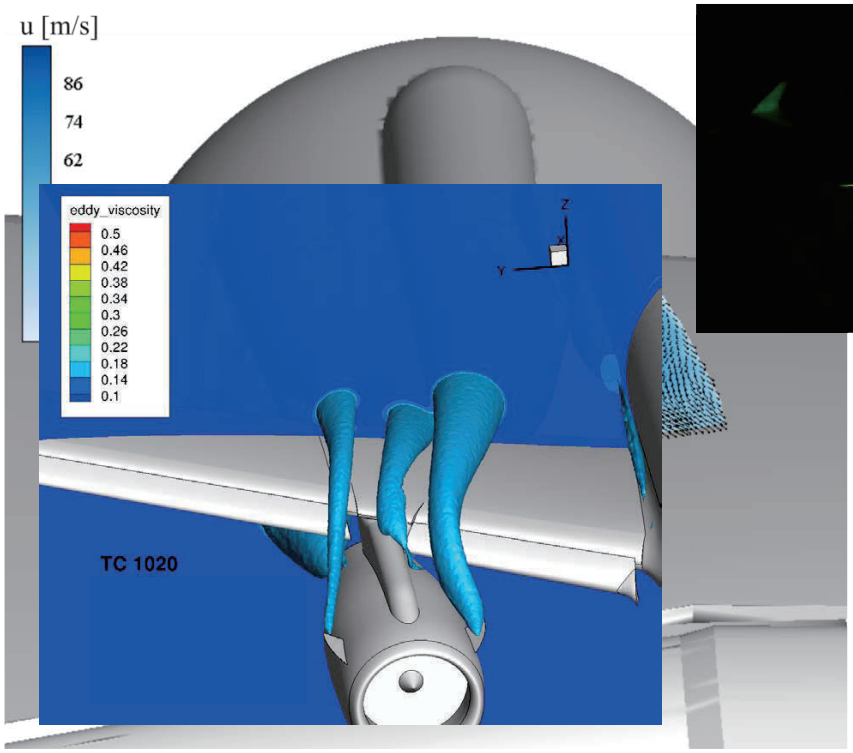


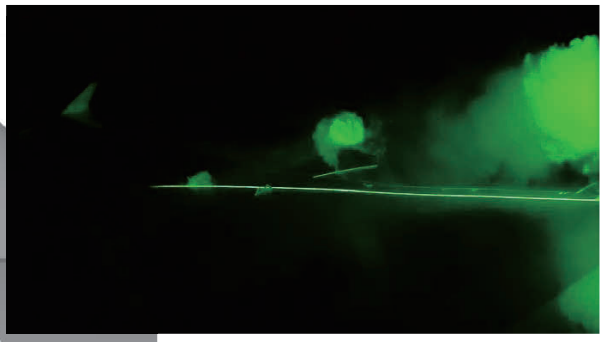

From left to right:
- slat track vortex
- outboard strake vortex
- inboard strake vortex

DLR.de • Chart 85 > L. Koop • High-Re Testing > July 7th 2016

## HINVA flight test #2: In-flight PIV

### PIV Results at FL100

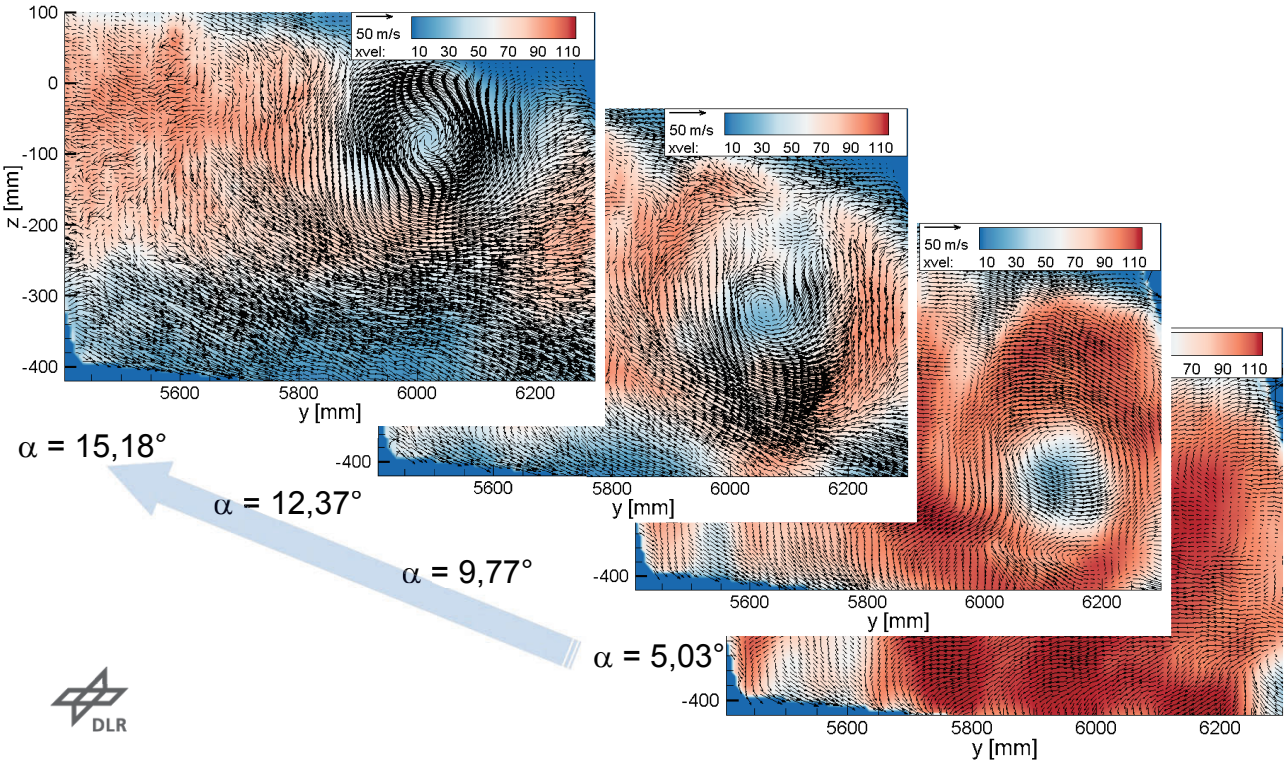


DLR.de • Chart 86 > L. Koop • High-Re Testing > July 7th 2016

## Summary; Chapter 4

- Provide data base at maximum lift through wind tunnel and flight tests
- Synergetic benefits from all three methods
- Deriving simulation strategy from obtained results

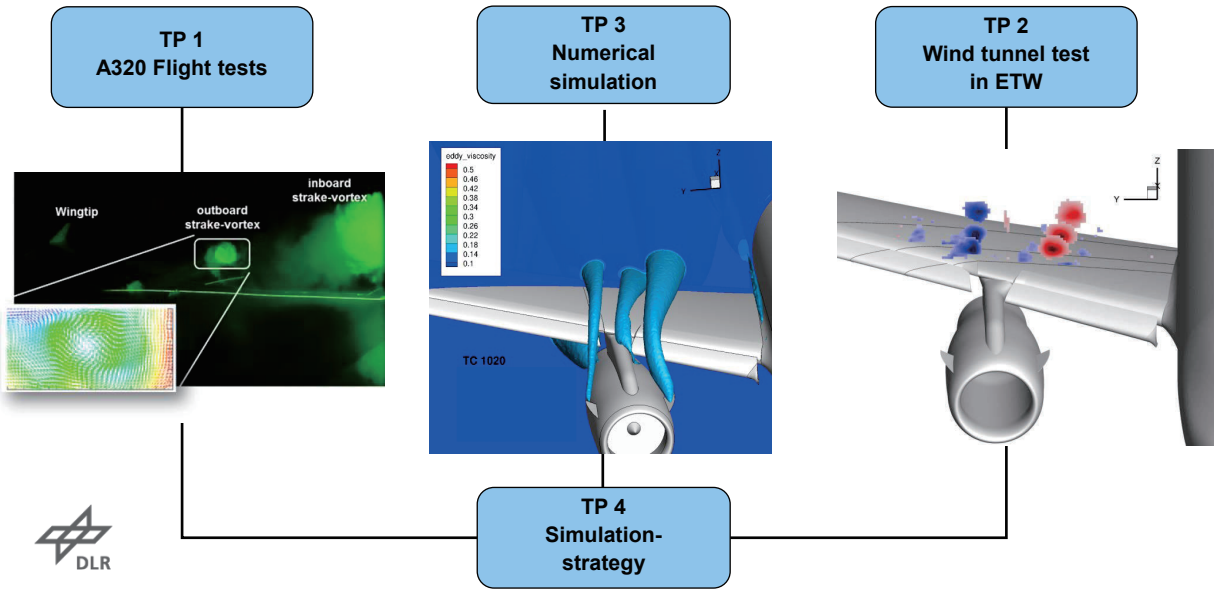

DLR.de • Chart 87 > L. Koop • High-Re Testing > July 7th 2016

## Summary

- Development towards high resolution measurement with optimal accuracy is mandatory for optical non intrusive measurement techniques
- High Reynolds number testing has become important during the last decade
  - Novel aircraft concepts
  - Physical understanding
  - Validation of numerical codes
- Transfer well established optimized optical measurement techniques to high Re testing
- Constant improvement in order to provide the best possible results for the adaptation, optimization and validation of numerical codes

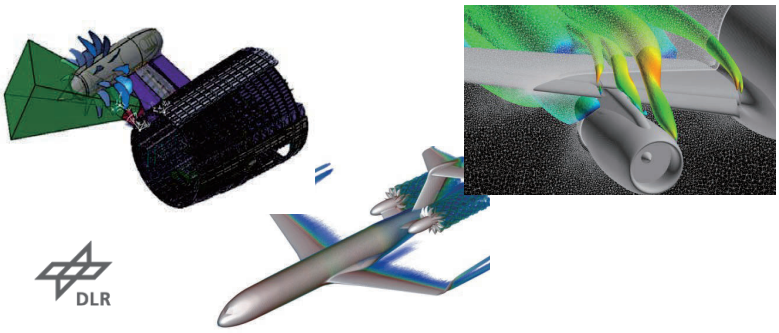

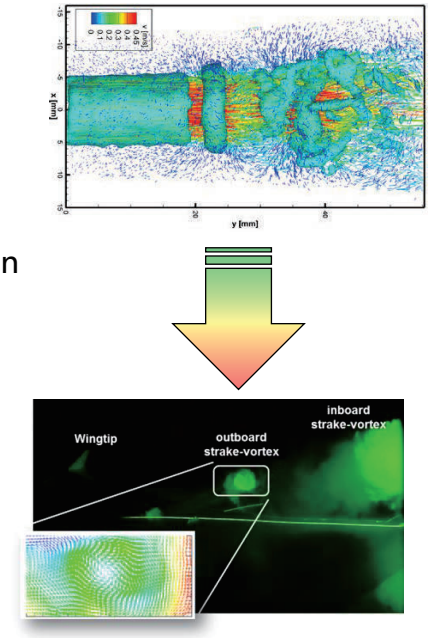


DLR.de • Chart 88 > L. Koop • High-Re Testing > July 7th 2016

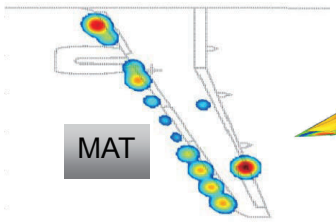


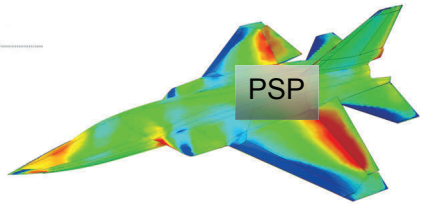


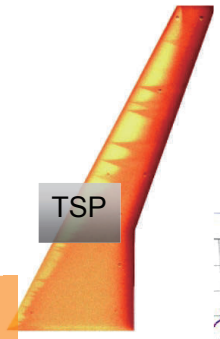


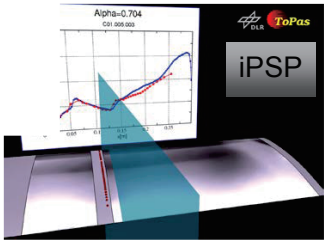



Thank you very much!

Lars Koop
Lars.koop@dlr.de
DLR Göttingen